NASA Technical Paper 2302

July 1984

Microstructure and Orientation Effects on Properties of Discontinuous Silicon Carbide/Aluminum Composites

David L. McDanels
and Charles A. Hoffman

NASA

NASA Technical Paper 2302

1984

Microstructure and Orientation Effects on Properties of Discontinuous Silicon Carbide/Aluminum Composites

David L. McDanels
and Charles A. Hoffman

Lewis Research Center
Cleveland, Ohio

National Aeronautics
and Space Administration

Scientific and Technical Information Branch

Summary

Composite panels containing up to 40 vol % discontinuous SiC whisker, nodule, or particulate reinforcement in several aluminum matrices were commercially fabricated and delivered to NASA Lewis for evaluation of mechanical properties and microstructural characteristics. The elastic modulus of the composites was found to be isotropic and independent of the type of reinforcement used and was controlled solely by the volume percentage of SiC reinforcement present. The yield and tensile strengths and the ductility were controlled primarily by the matrix alloy, the temper condition, and the reinforcement content. The type and orientation of reinforcement had some effect on the yield and tensile strengths of the composites, but only for those in which the whiskers were more highly oriented. The effect was not general. This suggests that, with the current state of the art in materials and fabrication development, particulate and nodule reinforcements are as effective as whisker reinforcement. Higher failure strains were observed in composites tested in this study than in most previous studies. This increase in ductility was attributed to purer, more uniform starting materials and to more mechanical working during fabrication. Comparing mechanical properties with those of other aluminum alloys showed that these low-cost, lightweight composites demonstrate very good potential for application to aerospace structures.

Introduction

Most of the research in aluminum matrix composites has been directed toward developing high-performance composites for use in specialized aerospace applications. For example, most of the aluminum matrix composite development at the NASA Lewis Research Center has been directed toward improving the impact resistance of boron/aluminum (B/Al) composites for possible application as rotating fan blades in aircraft engines. Because of the critical strength, stiffness, and impact requirements of such applications, it could be cost effective to use high-cost, high-performance composites for these components (ref. 1).

However, there are a number of other applications in aircraft engines and aerospace structures where the superior properties of high-performance composites may not be required and where it can be cost effective to use other metal matrix composites (fig. 1). For example, cost-, weight-, and stiffness-critical components, such as engine static structures and compressor vanes and blades, do not require the very high directional properties of B/Al. Replacing such current aluminum, titanium, or steel structures with composites offers the potential of significant weight and cost savings.

For these reasons, research was begun at NASA Lewis to assess the potential of low-cost aluminum matrix composite materials and low-cost composite fabrication processes (including powder metallurgy, direct casting, and hot molding techniques) for application to these structures (ref. 2). As part of this assessment, flat panels of low-cost aluminum matrix composites containing discontinuous silicon carbide whisker (SiC_w), nodule (SiC_n), or particulate (SiC_p) reinforcement were fabricated under contract. These panels were delivered to NASA Lewis for in-house evaluation of the suitability of these composites for the potential applications. Results from preliminary mechanical property testing of these discontinuous SiC/Al composites (ref. 2) indicated that these low-cost composites had significantly higher elastic moduli than conventional aluminum alloys and thus deserved further evaluation.

This current report presents the results of further analysis of the stress-strain and fracture behavior of these SiC/Al composites, with particular emphasis on the modulus, strength, ductility, and microstructural behavior observed. It also compares the properties observed with those that would be needed for these composites to be considered as viable candidates to replace current monolithic materials, such as titanium and aluminum, for aircraft engine component and structural applications.

Materials and Testing Procedures

Materials and Fabrication

Four commercial aluminum alloys were chosen as matrix alloys for the property studies of composites

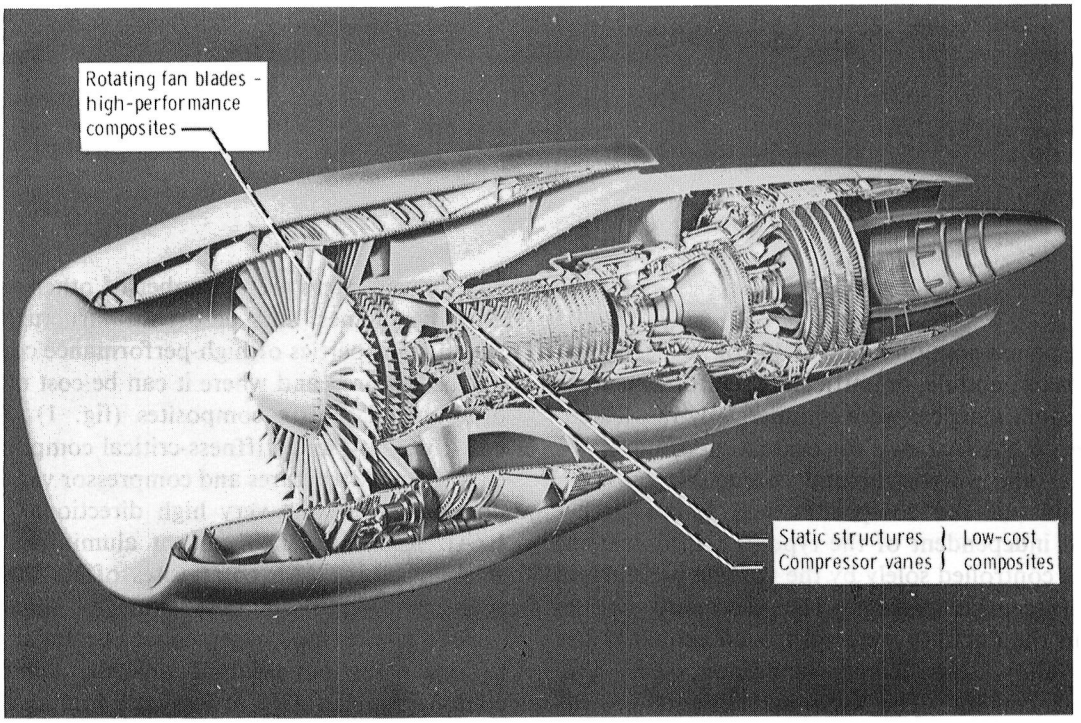

Figure 1.—Potential areas of application of aluminum matrix composites in aircraft gas turbine engines.

containing discontinuous SiC reinforcements. Alloy 6061 was chosen as the standard matrix alloy for comparison since it represented a class of heat-treatable alloys with high strength and ductility combined with good corrosion resistance and weldability. Two typical very high-strength aluminum alloys, 2024 and 7075, were also chosen. This class of alloy is heat treatable and is used in high-strength aerospace applications where corrosion resistance and weldability are of secondary importance. Alloy 2124 was used as the matrix for the 20 vol % SiC_w composites. However, the properties and characteristics of this alloy are almost identical to those of 2024 Al, so the two alloys were considered as one group throughout this study. Alloy 5083 was chosen as a matrix alloy to be typical of non-heat-treatable alloys that draw their moderate strength from work hardening. This alloy has good formability, weldability, and corrosion resistance. The handbook compositions and properties (ref. 3) of these alloys, in wrought form (table I), should approximate the properties attainable with the powder-metallurgy versions of the same alloys used as matrices for these composites.

Three types of low-cost, high-modulus aluminum matrix composite containing discontinuous SiC reinforcement have recently become commercially available and were studied in this investigation. Two types of this composite, containing SiC reinforcements produced from rice hulls (ref. 4), are being produced by ARCO Metals (formerly Silag Div. of Exxon Corp.). These composites contain either a predominantly SiC

TABLE I. - PROPERTIES OF UNREINFORCED WROUGHT ALUMINUM ALLOYS[a]

Alloy	Nominal composition	Density		Elastic modulus		Yield strength[b]		Ultimate tensile strength[b]		Failure strain[b], percent
		g/cm^3	lb/in^3	GPa	Msi	MPa	ksi	MPa	ksi	
2024 Al	4.5Cu-1.5Mg-0.6Mn	2.77	0.100	69.6	10.1	365	53	462	67	11
5082 Al	4.5Mg-0.7Mn	2.66	.096	71.0	10.3	228	33	317	46	16
6061 Al	1.0Mg-0.25Cu-0.25Cr-0.6Si	2.70	.098	69.0	10.0	276	40	310	45	17
7075 Al	5.5Zn-2.5Mg-1.5Cu-0.3Cr	2.80	.101	71.7	10.4	503	73	572	83	11

[a]From ref. 3.
[b]Optimum temper.

whisker reinforcement (Silag Grade F-9, containing a mixture of 80 percent whiskers and 20 percent nodules) or a predominantly SiC nodule reinforcement (Silag Grade X-0, containing a mixture of 80 percent nodules and 20 percent whiskers).

A third type of aluminum matrix composite, containing discontinuous SiC particulate reinforcement, is being produced by DWA Composite Specialties, Inc. This type of composite is made with SiC reinforcement obtained from single crystals of abrasive-grade SiC that have been crushed into fine powder and separated by size (ref. 5).

Basically the same methods were used to fabricate composites containing each of the three types of SiC reinforcement (refs. 5 and 6). In each case the SiC reinforcement was blended with aluminum alloy powder, compacted into billets, and sintered. In this investigation, billets were prepared, for the various matrix alloys and reinforcement types to be studied, with reinforcement contents ranging from 10 to 40 vol %. The sintered billets were extruded and then cross rolled into 2.54-mm (0.100-in.) thick flat plates and delivered to NASA Lewis for in-house evaluation. The nominal SiC reinforcement contents supplied by the fabricators were used throughout this study. No attempt was made to determine the actual reinforcement contents, as reference 5 indicated that the actual reinforcement contents were usually within ± 1 vol % of the nominal.

Property Evaluation

After the various SiC/Al plates had been received from both fabricators, the plates were oriented relative to their final rolling direction and then were sheared into 12.8-mm (0.5-in.) wide strips. One group was oriented parallel (longitudinal) to the final rolling direction; the other group was oriented perpendicular (transverse) to the final rolling direction. Tensile test specimens were made from these strips by milling a 28-mm (1.1 in.) long reduced-width test section.

Tensile tests were used to evaluate the stress-strain behavior and mechanical properties of the composites and to relate the effects of the type of SiC reinforcement, the SiC reinforcement content, the matrix alloy, and the temper condition on the modulus of elasticity, yield strength, ultimate tensile strength, and failure strain of the composites in both the longitudinal and transverse directions. Composites with 2024, 6061, and 7075 Al matrices were tested in both the as-fabricated (F temper) and the heat-treated (T6 temper) conditions. The heat treatments used (table II) were based on those given in reference 3. Composites with a 5083 Al matrix were tested in the F temper only. Tensile tests were conducted at room temperature at a constant crosshead speed of 0.508 mm/min (0.02 in/min), and the modulus and stress-strain behavior were determined by using a 25.4-mm (1.0-in.) gage length strain-gage extensometer.

A limited number of tensile tests were also conducted at temperatures to 316° C (600° F). Extensometers were not used for these tests and the stress-strain behavior was estimated from load-time curves. The specimen was allowed to stabilize at temperature within the testing furnace for about 10 min before each test.

After testing, the density of each type of composite was determined by the water immersion method. Two determinations were made on each type of composite, each using one-half of a failed tensile test specimen in the as-fabricated (F temper) condition. One determination was made on a specimen with a longitudinal orientation; the other, on a specimen with a transverse orientation.

SEM Metallographic Examination

The reinforcement distribution and fracture surfaces of each type of SiC/Al composite tested were examined by scanning electron microscopy (SEM). The cutting sequence and locations of the surfaces to be examined are shown schematically in figure 2. Samples containing the surfaces to be examined were prepared from failed tensile test specimens of each type of SiC/Al composite by using an abrasive wheel to cut off successive lengths of approximately 1 cm (0.39 in.) of material, starting at the fracture edge of the failed specimens. Each cut section was rinsed in tepid water and then ultrasonically cleaned in ethyl alcohol for about 5 min.

In the first set of SEM samples the top, side, and end surfaces were examined to determine the distribution and structure of the SiC reinforcement. In this case, after cutting and before mounting, the surfaces to be examined were heavily etched with HCl to remove some of the aluminum matrix in order to expose the SiC reinforcement below the original surface. Figure 3 shows

TABLE II. - HEAT TREATMENTS OF ALUMINUM MATRIX COMPOSITES

Alloy	Solution treatment[a]	Artificial aging[b]
2024 Al	482° C (900 °F) - 2 hr - WQ	177° C (350° F) - 24 hr - AC
6061 Al	527° C (980° F) - 2 hr - WQ	177° C (350° F) - 18 hr - AC
7075 Al	482° C (900° F) - 2 hr - WQ	121° C (250° F) - 24 hr - AC

[a]WQ = water quenched.
[b]AC = air cooled.

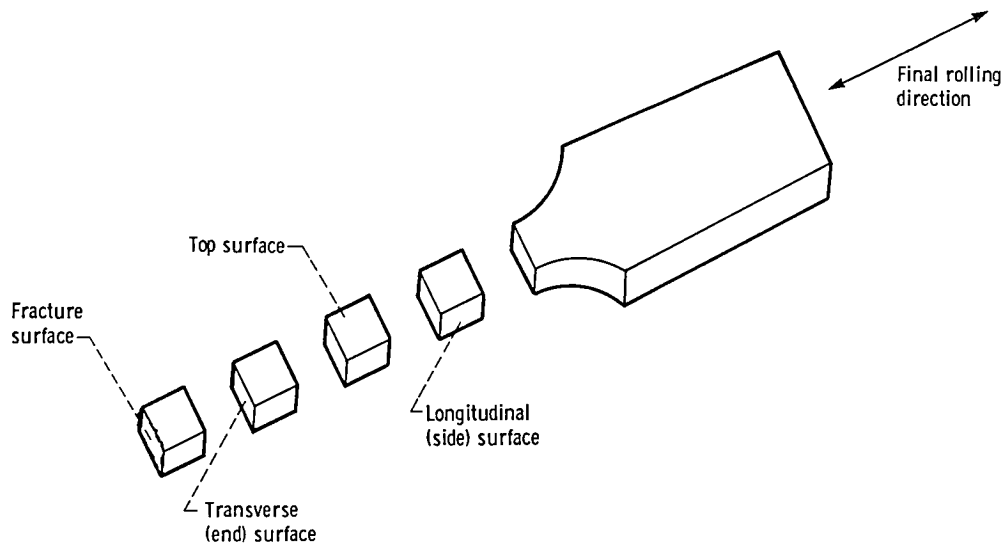

Figure 2.—Schematic diagram showing location of cuts made in fractured tensile test specimens to show various surfaces for SEM examination.

the surfaces of these composites during the etching process. Etching continued until several additional layers of reinforcement were exposed. After etching, the three cut sections from each specimen were positioned on a single aluminum mounting disk so that the sections showing the top, side, and end surfaces could be examined sequentially without the need to interchange mounts in the SEM. The surfaces of the specimen/mount units were coated with a thin CVD layer of gold, and then each specimen was positioned in the SEM at a 90° angle to the electron beam for examination.

Fracture surfaces of each type of composite were also examined, but these surfaces were not etched. Two fracture surface specimens were attached to each mount with adhesive-backed copper or aluminum tape. Fracture edge specimens were tilted at an angle of 90° to the electron beam and then offset 20° for examination.

Results

Structure of Discontinuous SiC/Al Composites

A series of 6061 Al matrix composites were studied to examine the structure of typical SiC/Al composites. Surfaces to be examined were heavily etched to allow the reinforcement distribution below the surface to be examined. After etching, the top, side, and end surfaces, relative to the rolling direction, were examined with SEM to show the size, shape, and distribution of the reinforcement. These surfaces are shown in figure 4 for composites containing 20 vol % of each type of reinforcement studied.

On the top surfaces of composites containing 20 vol % SiC_w reinforcement (fig. 4(a)) the whiskers have a somewhat random distribution, although there is a tendency for a general whisker orientation across the width dimension, perpendicular to the rolling direction. The side and end surfaces are similar in structure and have about the same amount of whiskers protruding from each etched surface. However, the end surface has a greater number of whiskers generally oriented in the width dimension, transverse to the final rolling direction, and the side surface has more whiskers projecting out of the etched surface, in the transverse direction.

The structure of a typical 20 vol % SiC_w/6061 Al composite (fig. 4(b)) indicates that three types of particles were present: whiskers, nodules, and agglomerates. Although the acicular whiskers appear to be equiaxed in cross section with a diameter between 0.2 and 0.9 mm, higher magnification shows these whiskers to be hexagonal. The whiskers tend to have a general orientation perpendicular to the final rolling direction. Some ribbon-like whiskers were observed as well. These are also hexagonal but are distorted to a much greater width than thickness. Some nodule reinforcement and some areas of differential etching were observed. The etching effects indicate either a difference in chemical composition or a difference in the internal strain state of these areas. It is probable that unstringered, agglomerated aluminum powder particles are present there. The less heavily worked areas of the composite would tend to be less anodic than the more heavily worked areas and thus would etch at a slower rate. The agglomerated areas had a matrix with SiC reinforcement projecting out at all angles. These areas could also be unwanted debris particles or aluminum-rich intermetallic inclusions.

The structure of a typical 20 vol % SiC_n/6061 Al composite (fig. 5) indicates that the reinforcement

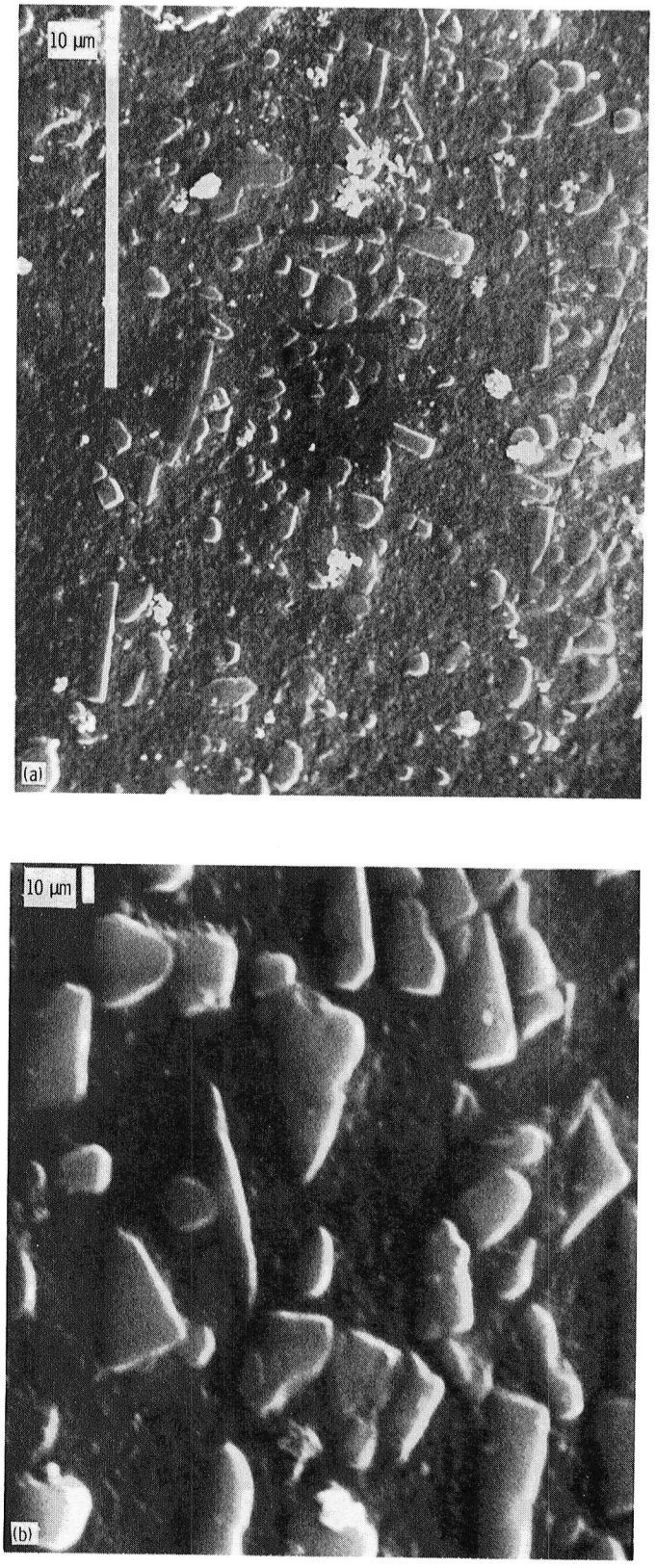

(a) 10 vol % SiC_w/6061 Al.
(b) 15 vol % SiC_p/6061 Al.

Figure 3.—Scanning electron microscope photographs of partially etched surfaces of SiC/Al composites.

consists predominantly of SiC nodules. These nodules are similar to those seen with the SiC_w reinforcement. The nodules are smooth-surfaced, irregularly shaped platelets, 1 to 5 μm in size, equiaxed in cross section, and generally with a thickness of about half the diameter. A few whiskers were visible, again with a generally transverse orientation; in addition, some agglomerates were visible. The structures of the side and end surfaces are similar to that of the top surface.

The structure of a typical 20 vol % SiC_p/6061 Al composite (fig. 6) indicates that the SiC_p reinforcement is very angular and has an irregularly jagged wedge shape. Most of the SiC_p reinforcement ranges in size from 2 to 7 μm. Fewer agglomerates are present in the SiC_p/Al composites than in the SiC_w and SiC_n composites. Views of the surfaces of these composites show the particulates to be randomly oriented. The distribution in the top view shows more reinforcements than the other surfaces, but this is caused by the etching action. On the top surface the wedge-shaped particulates can be trapped by adjacent particulates still partially bonded to the matrix, but on the end and side surfaces the particulates would tend to fall out if the etch undercut the supporting matrix at the embedded ends.

As the reinforcement content increased, the reinforcement packing became denser and the distance between reinforcing particles became smaller. The SiC_p reinforcements appear similar in composites containing 15 to 30 vol % reinforcement; however, the 40 vol % SiC_p/6061 Al composites have much larger particulates than the other SiC_p composites. These SiC_p particulates are more like platelets than the nodules or whiskers and range in size to 10 by 21 μm across the extreme axes of the visible dimensions.

The packing, as demonstrated by the end view, is also much denser, and the faces of most of the particulates touch. The distribution gives the appearance of a "cut fieldstone fence" stacking. The buildup of this stacked structure is shown more clearly by the end views of the 30 and 40 vol % SiC_p/6061 Al composites (fig. 7). Composites with 30 vol % SiC_p reinforcement have dense packing but still have free areas of matrix around the SiC_p reinforcement. The larger particulates of the 40 vol % SiC_p composites show the fence-like stacking of the flatter SiC_p reinforcement, with adjacent particulates touching and a minimum of matrix available between particulates.

Properties of Discontinuous SiC/Al Composites

Room-temperature tensile tests were conducted on specimens of discontinuous SiC/Al composites having orientations parallel or perpendicular to the final rolling direction. Where applicable, tensile tests were conducted on the SiC/Al composites in both the as-fabricated (F temper) and heat-treated (T6 temper) conditions.

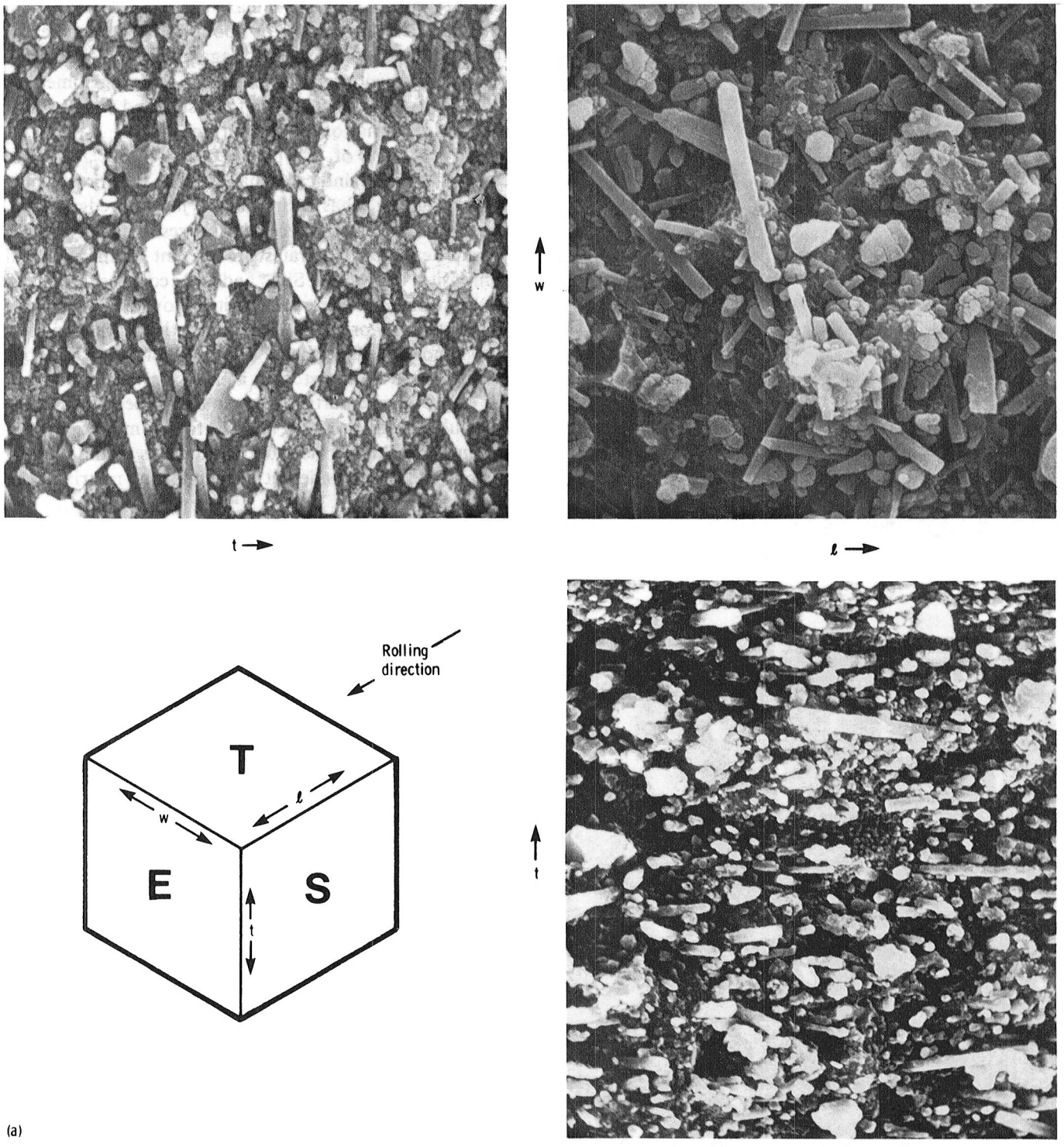

(a)

(a) Structure of each surface.

Figure 4.—Structure of typical etched 20 vol % SiC_w/6061 Al composite.

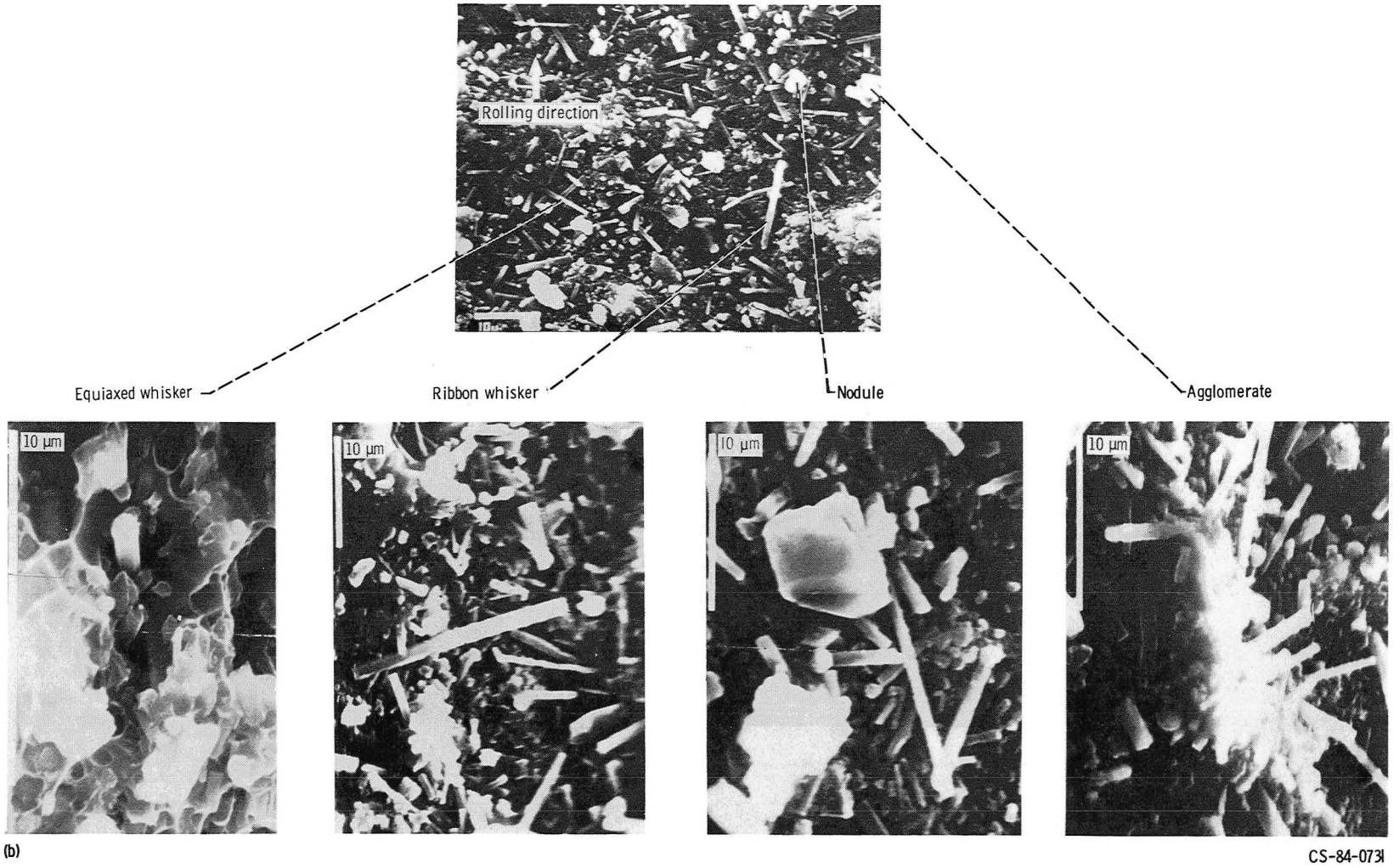

(b) Details of structure of top surface.

Figure 4.—Concluded.

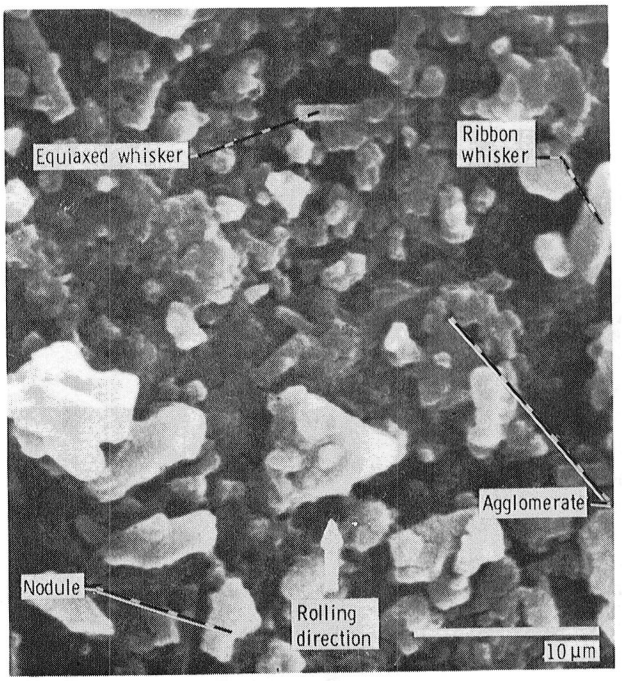

Figure 5.—Structure of typical SiC_n/6061 Al composite (top surface).

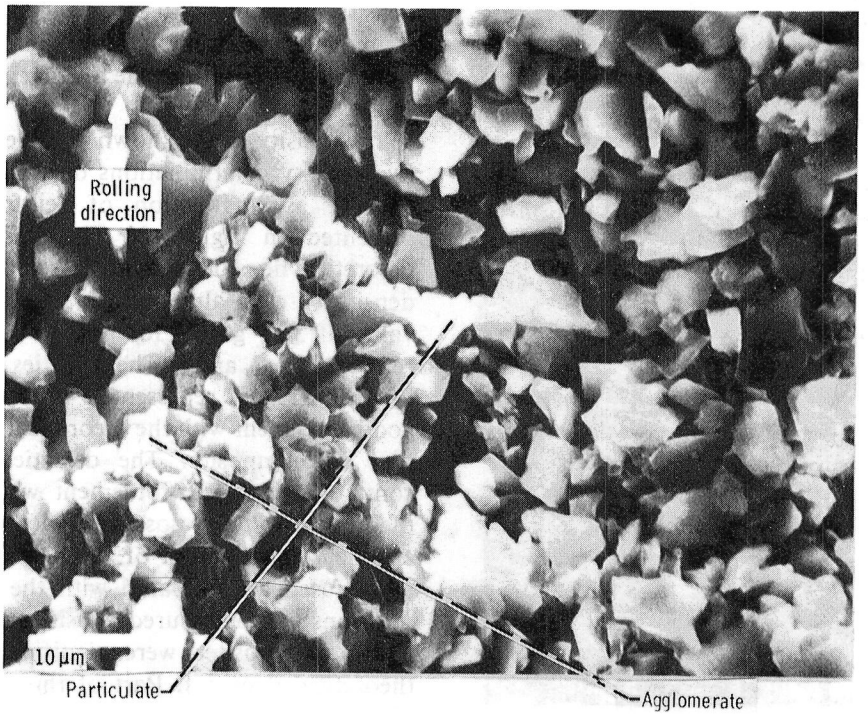

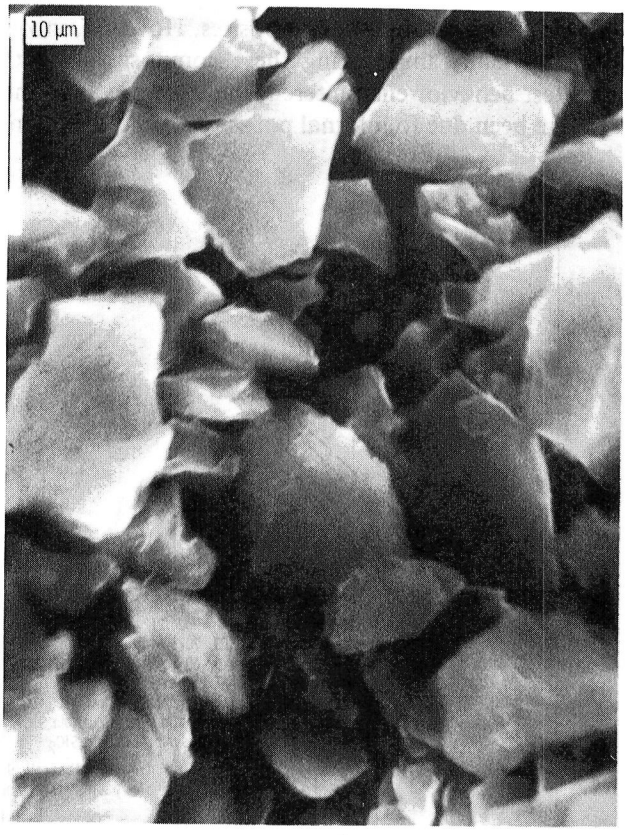

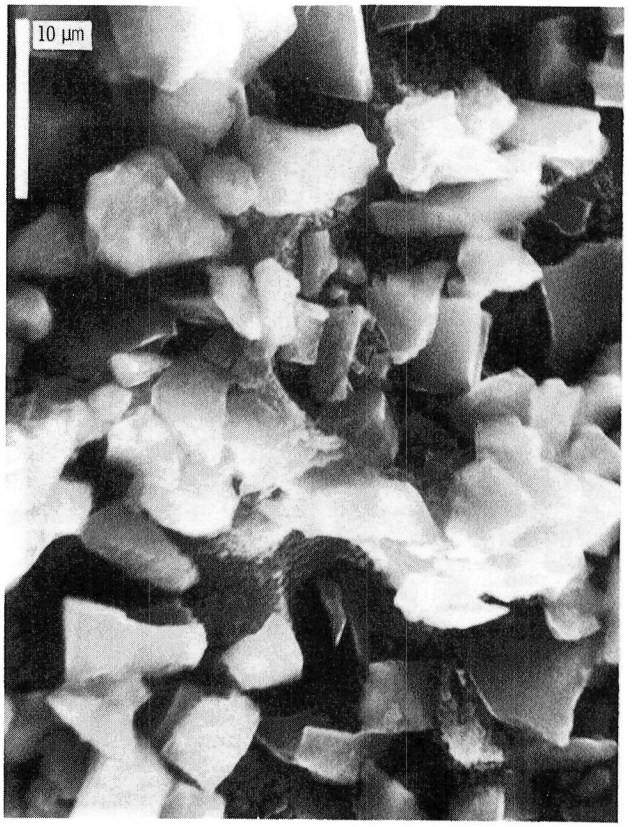

Figure 6.—Structure of typical SiC_p/6061 Al composite (top surface).

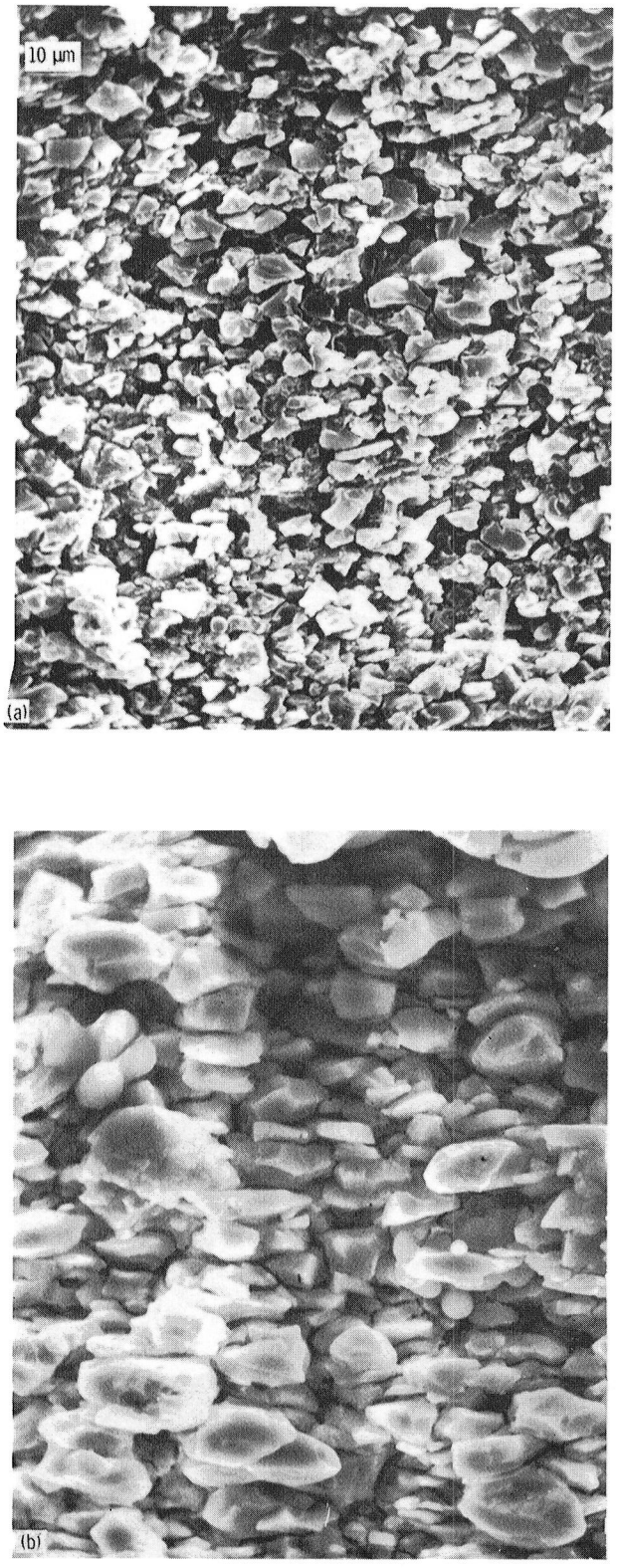

(a) 30 vol % SiC_p.
(b) 40 vol % SiC_p.

Figure 7.—Structure of etched end surface of typical SiC_w/6061 Al composite.

The results of density and tensile tests conducted on SiC/Al composite specimens are summarized in table III for each type of composite studied. The average values of density, modulus, 0.2-percent-offset yield strength, ultimate tensile strength, and failure strain are tabulated. These values represent the average of two to six tests for each category.

The density values shown in table III are an average of two density determinations on each type of composite. Density as a function of reinforcement content is presented in figure 8. The dashed lines represent theoretical densities that are based on the rule-of-mixture density of each aluminum matrix alloy (ref. 3) and the value of 3.21 g/cm^3 for both α and β-SiC reported in references 5, 7, and 8. The densities measured for most of the composites, represented by the data points, show good agreement with the theoretical density lines for each type of composite. The densities of the composites containing SiC_p reinforcement were slightly below the theoretical value, a possible indication of changes in the chemical composition of the powder-metallurgy matrix alloys used as compared with the wrought alloy compositions. The measured densities of all of the 5083 Al matrix composites were significantly lower than the theoretical densities. Part of this effect may be due to alloy composition variations in the powder-metallurgy 5083 Al used to make these composites. However, in view of the difficulty in shearing these composites and the brittle test behavior encountered, these lower values may also have been due to internal porosity or microcracking,

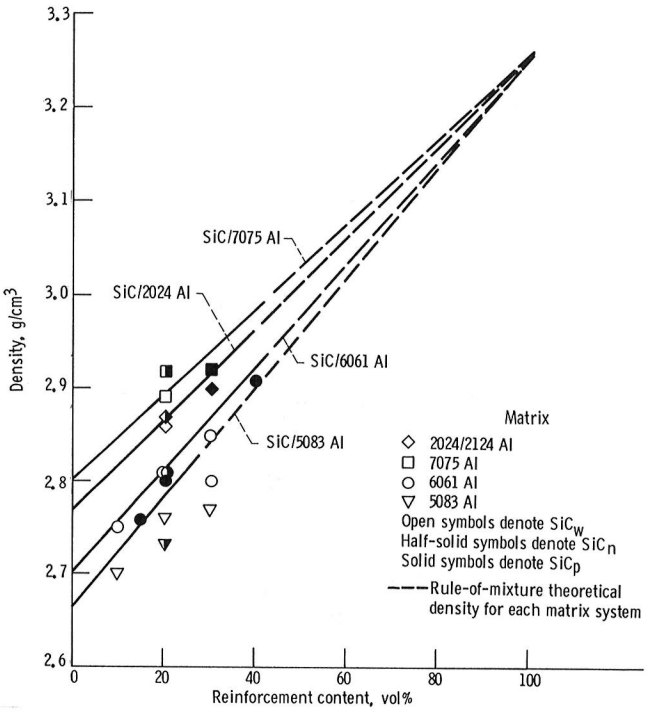

Figure 8.—Measured typical and theoretical densities for SiC/Al composites.

TABLE III. - SUMMARY OF RESULTS FROM DISCONTINUOUS SiC-REINFORCED ALUMINUM COMPOSITES

Alloy	SiC content, vol %	Type of SiC reinforcement[a]	Temper[b]	Density		Longitudinal direction							Transverse direction						
				g/cm^3	lb/in^3	Elastic modulus		Yield strength		Ultimate tensile strength		Failure strain, percent	Elastic modulus		Yield strength		Ultimate tensile strength		Failure strain, percent
						GPa	Msi	MPa	ksi	MPa	ksi		GPa	Msi	MPa	ksi	MPa	ksi	
6061	10	W	F	2.75	0.099	77	11.2	141	20.5	250	36.3	12.1	83	12.1	149	21.6	263	38.2	9.1
			T6			83	12.0	311	45.0	373	54.1	7.1	82	11.9	314	45.6	383	55.5	7.6
	15	P	F	2.76	.100	81	11.8	121	17.6	215	31.2	11.3	85	12.3	131	19.0	222	32.2	8.5
			T6			90	13.1	295	42.8	359	52.0	5.5	88	12.8	301	43.7	353	51.2	5.2
	20	W	F	2.81	.101	106	15.4	208	30.2	317	46.0	5.4	103	14.9	207	30.0	340	49.3	6.0
			T6			96	13.9	321	46.6	423	61.4	6.7	99	14.4	336	48.7	444	64.4	5.6
	20	N	F	2.81		103	14.9	168	24.4	261	37.8	9.3	103	14.9	168	24.3	264	38.3	8.0
			T6			99	14.3	316	45.9	385	55.9	5.6	97	14.1	329	47.7	424	61.5	4.3
	20	P	T6	2.80		108	15.7	356	51.6	428	62.1	4.9	101	14.7	348	50.5	406	58.9	4.3
	30	W	F	2.80		112	16.3	334	48.4	406	58.9	1.7	119	17.3	314	45.6	417	60.5	1.3
			T6			110	16.0	309	52.2	406	58.9	1.2	109	15.8	373	54.1	421	61.1	1.0
	30	P	F	2.85	.103	112	16.2	222	32.2	329	47.7	3.0	114	16.5	221	32.1	328	47.5	2.5
			T6			118	17.1	382	55.4	439	63.6	1.3	123	17.9	394	57.2	464	67.3	2.6
	40	P	T6	2.91	.105	134	19.4	428	62.1	457	66.3	.6	141	20.4	421	61.0	461	66.9	.8
2124	20	W	F	2.86	.103	105	15.2	315	45.7	455	66.0	4.0	106	15.3	312	45.2	505	73.3	2.4
			T6			96	14.0	388	56.3	535	77.6	3.8	102	14.8	388	56.3	587	85.2	2.9
2024	20	N	F	2.87	.104	103	15.0	240	34.8	345	50.1	2.7	106	15.3	243	35.3	362	52.5	2.4
			T6			95	13.8	350	50.8	445	64.5	3.2	102	14.8	352	51.0	452	65.5	3.1
	30	P	T6	2.90	.105	118	17.2	405	58.7	456	66.1	.8	115	16.7	401	58.2	464	67.3	.9
7075	20	W	F	2.89	.104	94	13.7	353	51.2	476	69.1	3.9	102	14.8	336	48.7	464	67.3	2.8
			T6			101	14.7	407	59.1	549	79.7	3.5	110	16.0	414	60.0	632	91.6	3.5
	20	N	F	2.92	.105	99	14.3	422	61.2	503	73.0	2.6	101	14.7	416	60.3	496	71.9	1.7
			T6			107	15.5	388	56.2	512	74.3	6.1	99	14.3	362	52.5	487	70.6	6.1
	30	P	F	2.92	.105	120	17.4	407	59.1	408	59.1	.6	117	17.0	379	54.9	441	63.9	1.0
			T6			119	17.3	392	56.8	439	63.7	.9	114	16.6	372	53.9	409	59.3	.7
5083	10	W	F	2.70	.098	86	12.5	214	31.1	285	41.3	3.3	89	12.9	223	32.3	304	44.1	2.6
	20	W	F	2.76	.100	100	14.5	312	45.3	352	51.0	.8	100	14.5	327	47.4	374	54.2	1.0
	20	N	F	2.73	.099	100	14.4	252	36.5	289	41.9	1.3	104	15.0	250	36.3	299	43.3	1.3
	30	W	F	2.77	.100	114	16.6	(c)	(c)	285	41.3	.4	125	18.1	370	53.6	376	54.6	.6

[a]W = SiC whiskers; N = SiC nodules; P = SiC particulates.
[b]F = As-fabricated condition; T6 = Heat-treated condition.
[c]No data.

although there was no evidence of this in the SEM examination.

Stress-strain curves of SiC/Al composites are summarized in figure 9 for each aluminum matrix alloy tested. These stress-strain curves, along with the results summarized in table III, show that the modulus of elasticity increased with increasing reinforcement content for each alloy. Also, in general, the yield and ultimate tensile strengths of the composites increased with increasing reinforcement content, but the failure strain decreased.

Results of a limited number of tensile tests conducted at temperatures up to 316° C (600° F) are presented in figure 10 for 20 vol % SiC_w/6061 Al composites tested in the longitudinal direction. The data at room temperature represent the average of several tests. The data shown for unreinforced 6061 Al are from reference 3.

Fracture Surfaces of SiC/Al Composites

Fracture surfaces of each type of SiC/Al composite tested in this investigation were examined by SEM metallography. The trends observed in the fracture surface examination are summarized by the microstructures presented in figures 11 to 14. The failure strain of each composite is indicated for each photograph. At low reinforcement contents (10 to 15 vol % SiC) a chisel-point shear fracture was observed, with a corresponding fine, lacy dimple network in the fracture surface (fig. 11). At intermediate reinforcement contents (20 vol % SiC) a transition type of fracture was observed with either a V-shaped double shear lip, in which one shear lip intersected another, or a shear lip-flat surface, in which the shear lip intersected a flat, granular plane. The first case gave a fracture surface with a coarser dimple network (fig. 12). The second case gave a fracture surface with a dimple/cleavage transition (fig. 13). At higher reinforcement contents (30 to 40 vol %), the specimens failed with a flat, granular fracture and had a corresponding cleavage type of granular fracture surface (fig. 14).

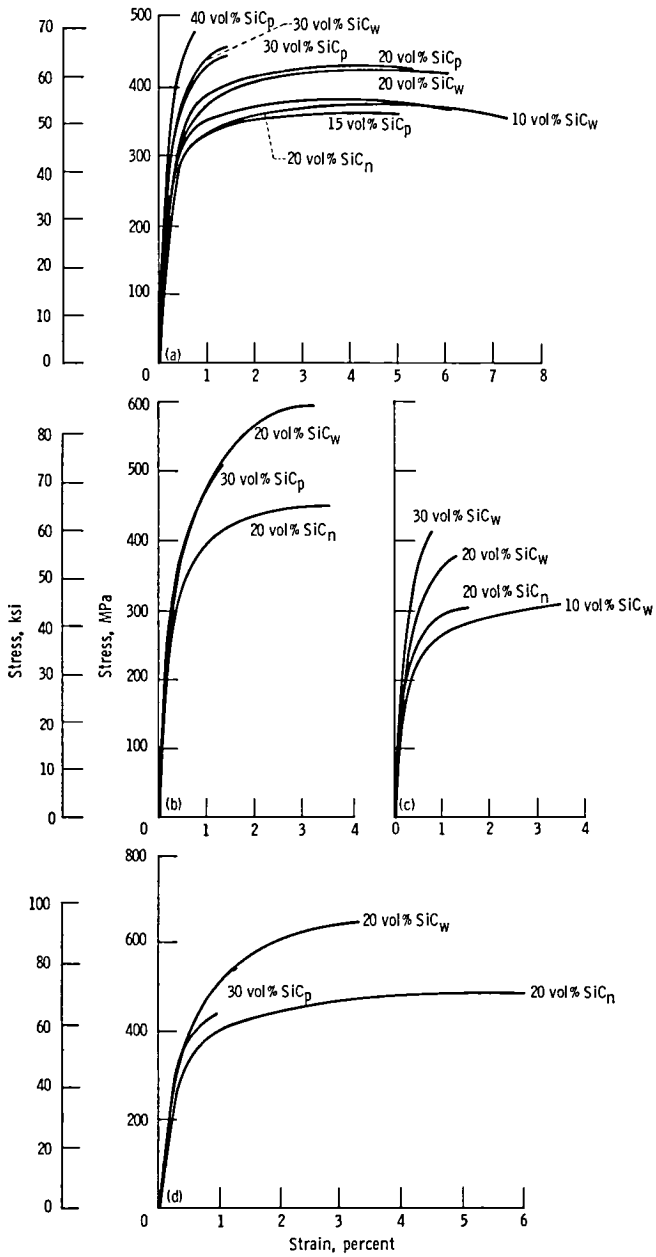

(a) SiC/6061 Al composites (T6 temper) tested in longitudinal direction.
(b) SiC/2024/2124 Al composites (T6 temper) tested in transverse direction.
(c) SiC/5083 Al composites (F temper) tested in transverse direction.
(d) SiC/7075 Al composites (T6 temper) tested in transverse direction.

Figure 9.—Stress-strain curves of SiC/Al composites.

Discussion

Factors Influencing Modulus of Elasticity of Discontinuous SiC/Al Composites

The results tabulated in table III are plotted in figure 15 to show the effect of the type and content of SiC

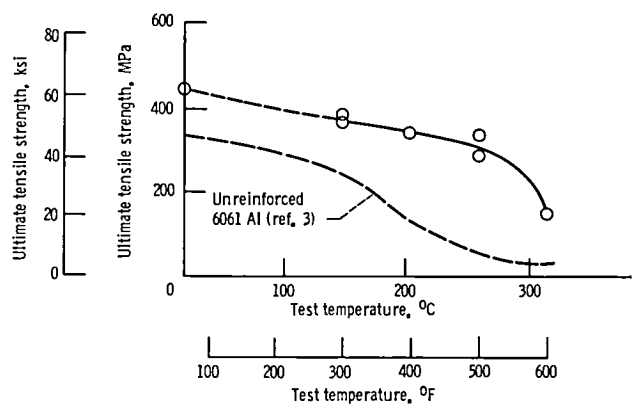

Figure 10.—Effect of test temperature on tensile strength of 20 vol % SiC_w/6061 Al composites.

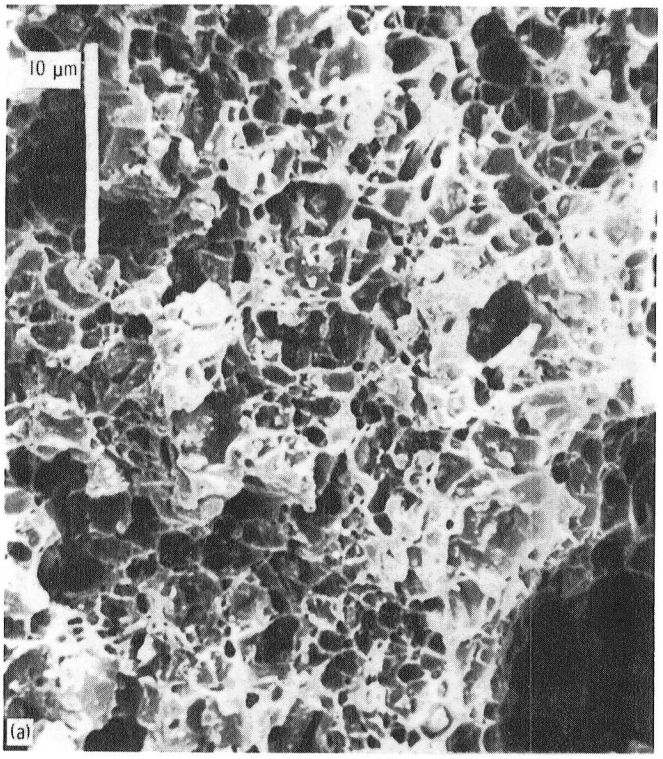

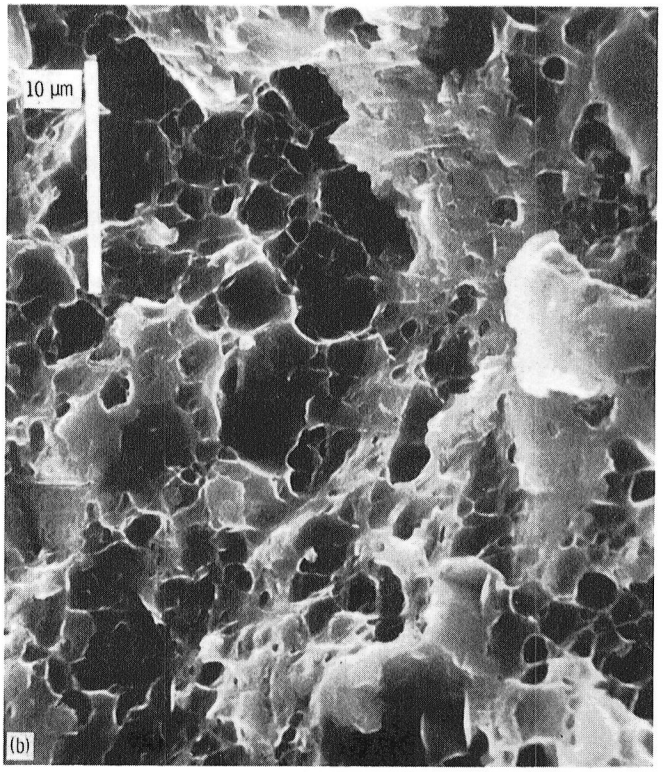

(a) Longitudinal orientation; failure strain, 12.0 percent.
(b) Transverse orientation; failure strain, 9.1 percent.

Figure 11.—SEM fracture surfaces of 10 vol % SiC_w/6061 Al composite, showing ductile fracture behavior.

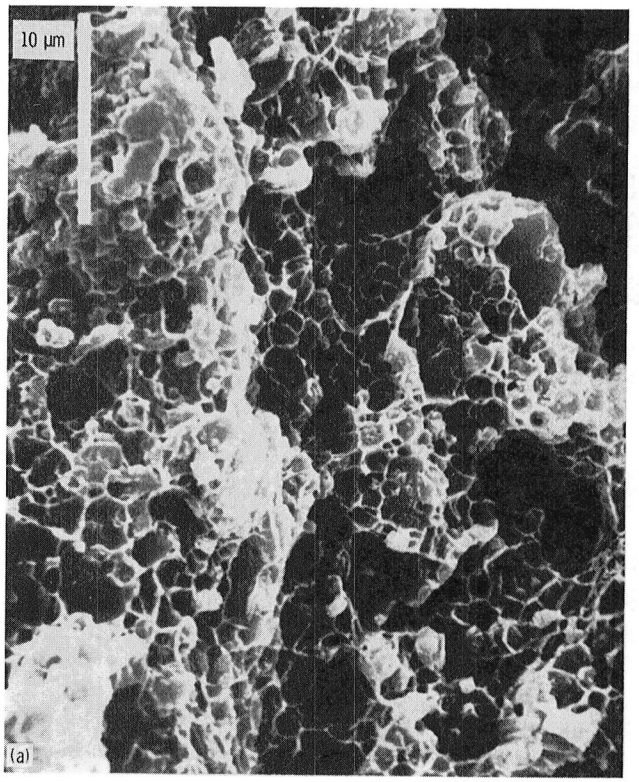

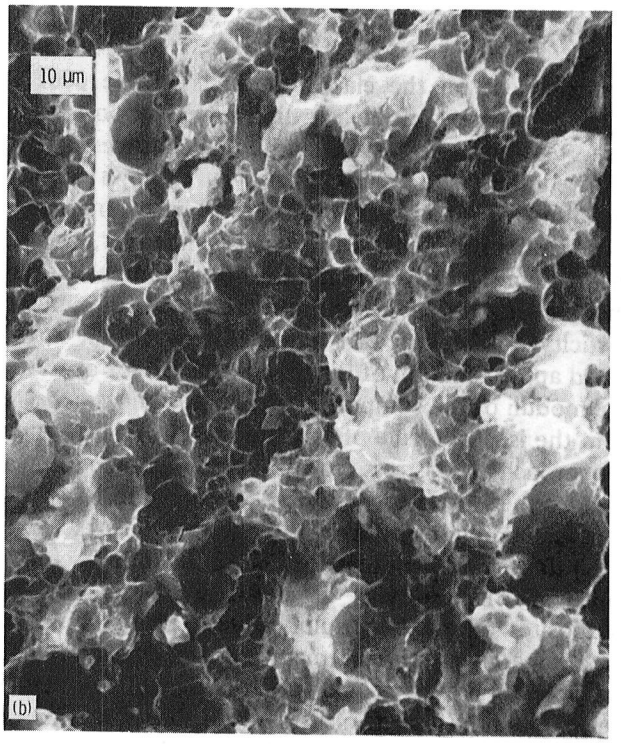

(a) Longitudinal orientation.
(b) Transverse orientation.

Figure 12. – SEM fracture surfaces of 20 vol % SiC_w/6061 Al composite, showing transitional fracture behavior with double shear lip. Failure strain, 5.3 percent.

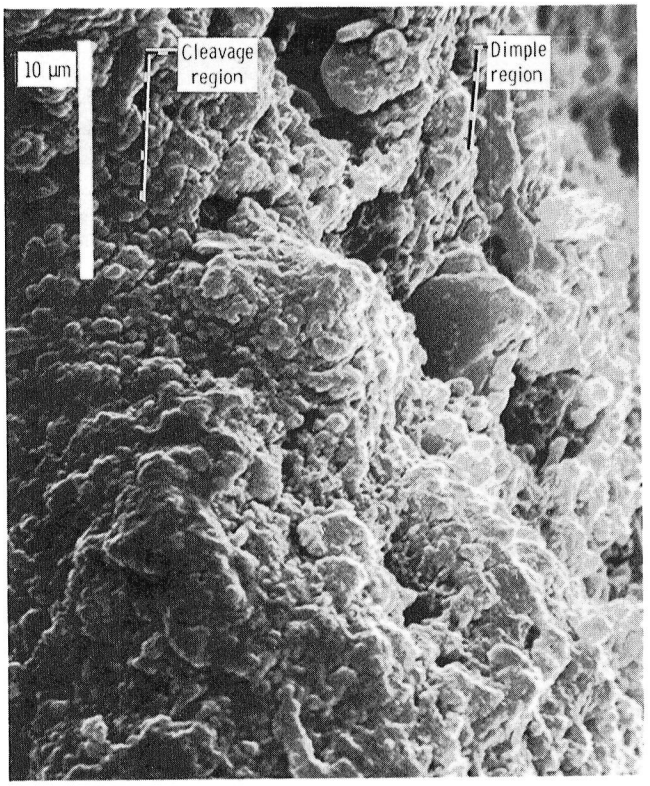

Figure 13.—SEM fracture surfaces of 20 vol % SiC_w/7075 Al composite, showing transitional fracture behavior with shear lip–flat surface intersection. Longitudinal orientation; failure strain, 3.2 percent.

reinforcement on the elastic modulus of the 6061 Al matrix composites studied in this investigation. Results from tests on the other aluminum matrices studied followed the same trends. This figure shows that the modulus of elasticity increased with increasing reinforcement content. This increase, however, was not linear, as in the case of continuous fiber composites with fibers aligned in the testing direction. The modulus of elasticity was replotted in figure 16 to show an extrapolated approximation of the modulus behavior observed. The moduli of the composites were below those expected from the isostrain rule-of-mixtures behavior and tended to approach an isostress type of hyperbolic function with reinforcement content, similar to that observed for transverse modulus behavior of fiber composites.

Reinforcement content is the dominant factor in improving the modulus of elasticity of these SiC/Al composites. Average modulus values (table III) indicate that, for a given reinforcement content, the modulus is isotropic, with nearly equal values obtained from tests in the longitudinal and transverse directions. In addition, the modulus is independent of the type of reinforcement, with modulus values being within 5 percent of the average for all composites tested at a given reinforcement content regardless of the type of reinforcement. To date, no results have been reported for the elastic moduli of SiC

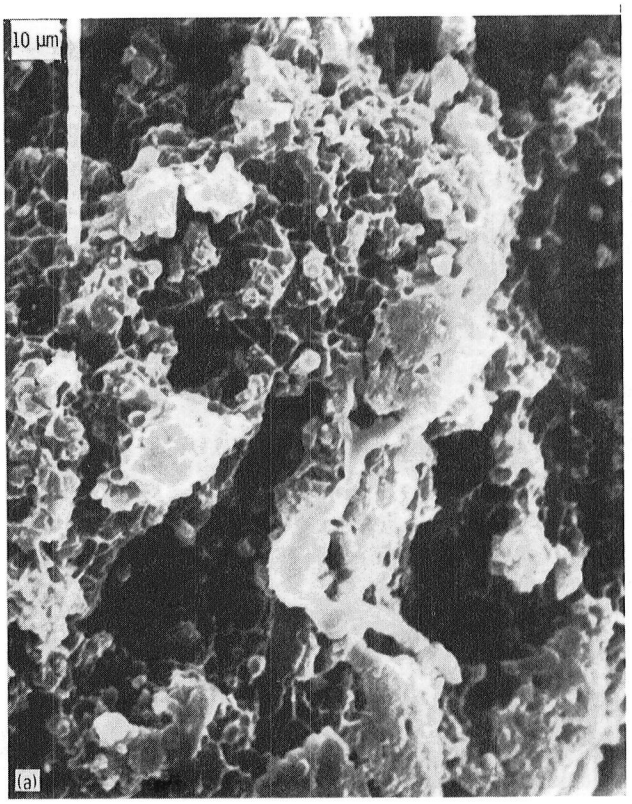

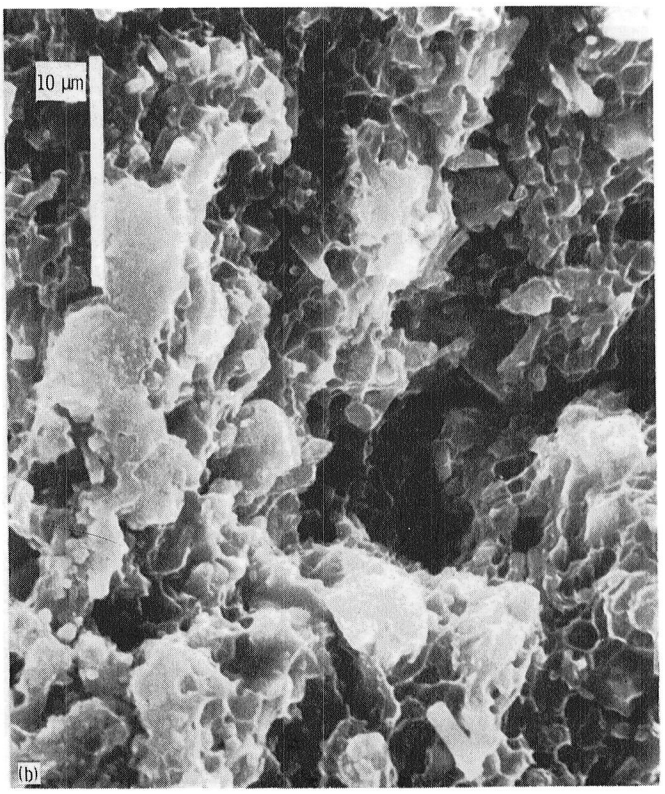

(a) Longitudinal orientation; failure strain, 2.6 percent.
(b) Transverse orientation; failure strain, 1.2 percent.

Figure 14.—SEM fracture surfaces of 30 vol % SiC_w/6061 Al composite, showing brittle fracture behavior.

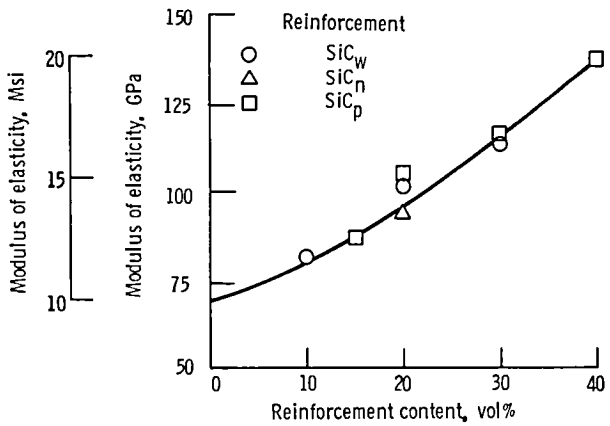

Figure 15.—Effect of reinforcement content on modulus of elasticity of discontinuous SiC/6061 Al composites.

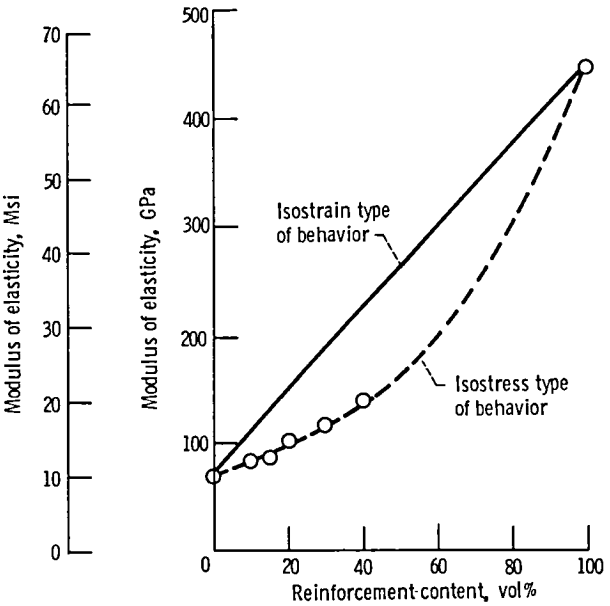

Figure 16.—Theoretical approximation of effect of reinforcement content on modulus of elasticity of discontinuous SiC/Al composites.

whiskers grown from rice hulls. The small diameters and short lengths of these whiskers make testing very difficult. Data reported many years ago showed that SiC whiskers had an elastic modulus of about 689 GPa (100 Msi), but those whiskers were grown and harvested by different processes than was used for the rice hull whiskers. Although the crystallographic orientation of whisker growth may give higher modulus, the rice hull whiskers were also smaller in diameter and their properties may be different from those reported previously.

The moduli of the composites were also independent of the matrix alloy. Heat treating the composites may have had a slight effect on modulus. The moduli of composites in the heat-treated (T6 temper) condition appeared to be slightly lower than the moduli measured on composites in the as-fabricated (F temper) condition. This reduction was slight (about 3 to 4 percent), was not consistent among all of the matrix alloys tested, and may have been due to scatter in the data.

Factors Influencing Strength of Discontinuous SiC/Al Composites

Because the factors influencing the yield and tensile strengths of SiC/Al composites are complex and interrelated, these strengths can best be evaluated by isolating the variables and analyzing the stress-strain curves and the fracture behavior. The stress-strain curves (summarized in fig. 9) are used for comparing tensile behavior.

Effect of aluminum matrix alloy.—The aluminum matrix used for discontinuous SiC/Al composites is the most important factor affecting the strength of these composites. The yield and ultimate tensile strengths of SiC/Al composites of a given reinforcement content are controlled primarily by the matrix alloy and heat treatment temper used. Although tests were conducted on composites in the both the F and T6 tempers in this study, in commercial usage the composites would probably be used almost exclusively in the heat-treated condition. Therefore most of the following discussion is based on the behavior observed on composites in the T6 temper.

To show this dependence on the aluminum matrix alloy, the effect of different matrix alloys on the stress-strain behavior of SiC/Al composites is summarized in figure 17. The stress-strain curves are shown for typical composites containing different aluminum matrix alloys but with the other parameters held constant. In this case, 20 vol % SiC_w reinforcement, T6 temper (where applicable), and testing in the longitudinal direction were

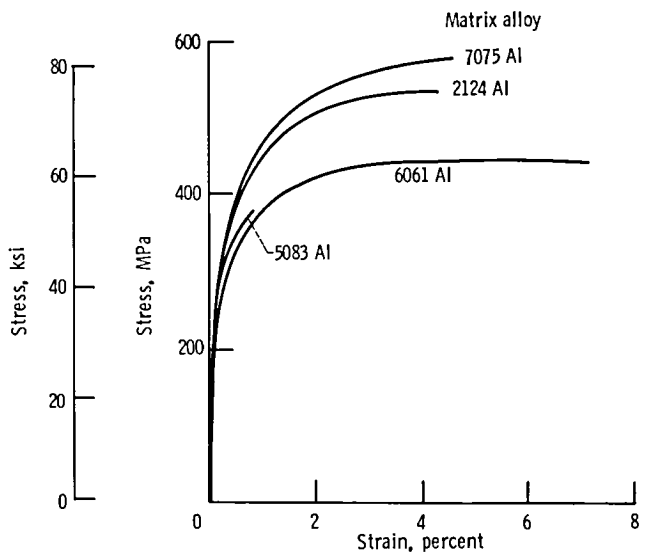

Figure 17.—Effect of aluminum matrix alloy on stress-strain behavior of heat-treated composites with 20 vol % SiC reinforcement. (Tested in direction parallel to final rolling direction.)

used as the analysis conditions. These curves show that SiC/Al composites with higher strength matrix alloys, such as 2024/2124 or 7075 Al, had higher strengths but lower ductilities. Composites with a 6061 Al matrix showed good strength and higher ductility. Composites with a 5083 Al matrix failed at lower strengths and in a brittle manner at a strain of less than 1 percent. The 5083 Al alloy is not heat treatable and has been developed to gain maximum properties in the strain-hardened H temper. The composition has been optimized to achieve maximum solid solution strengthening, and adding the SiC reinforcement probably overstrains the lattice. Thus there is not sufficient ductility left in the alloy for it to gain its potential strength and ductility.

The effect of heat treatment on the stress-strain behavior and tensile properties can also be seen in the results presented in table III. These results have been summarized in figure 18 to show the effect of heat treatment on SiC_w/6061 Al composites tested in the longitudinal direction. These stress-strain curves show that heat treatment significantly increased the yield and tensile strengths of the composites at all reinforcement contents tested. Although heat treatment had little, if any, effect on the modulus of elasticity of the composites, it did affect the transition into plastic flow. Composites in the as-fabricated (F temper) condition strained elastically and then passed into a normal decreasing-slope plastic flow. Composites tested in the T6 temper exhibited a slightly greater amount of elastic strain, with the elastic proportional limit being increased from about 0.10 to 0.15 percent strain to about 0.15 to 0.25 percent. However, the greater influence was a steepening of the slope of the stress-strain curve at the inception of plastic flow relative to that observed for composites in the F temper. The inception of plastic flow was marked by a continuation of a slope that, while no longer elastic and starting to become plastic, approached

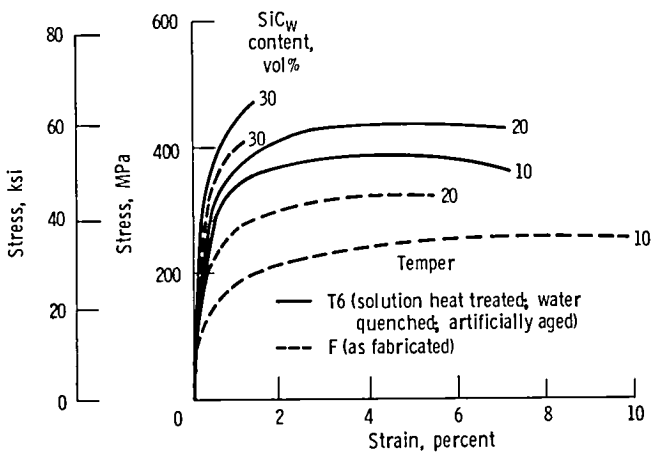

Figure 18.—Effect of heat treatment on stress-strain behavior of SiC_w/6061 Al composites.

that of the elastic portion. This slope decreased with increasing strain, until eventually it reached normal plastic flow and fractured at the ultimate tensile strength.

This steepening of the stress-strain curve and slight increase in elastic proportional strain limit (e.g., fig. 18) is reflected by the higher 0.2-percent-offset yield and ultimate tensile strengths observed for the heat-treated composites. The increase in flow stress of composites with each heat-treatable matrix probably reflects the additive effects of dislocation interaction with both the natural alloy precipitates and the added synthetic SiC reinforcement. This combination increased the lattice strain in the matrix, caused greater dislocation tangling, and required higher flow stresses for deformation.

To show the effect of matrix alloy and heat treatment on strength, the results are plotted in figure 19(a) as a histogram summarizing the effects of matrix alloy and heat treatment on the 0.2-percent-offset yield strength of typical SiC/Al composites. Figure 19(b) shows a similar histogram for ultimate tensile strength. Results are plotted for composites containing 20 vol % SiC_w reinforcement, in both the F and T6 tempers. These histograms are also typical of properties observed for other reinforcement contents. The properties for the unreinforced matrix alloys were taken from the maximum strength tempers listed in reference 3. These plots represent the average values obtained from all tests on composites of each matrix alloy with 20 vol % SiC_w reinforcement and show that the yield and ultimate tensile strengths of the SiC/Al composites were increased significantly by heat treatment. The plots also show that the strengths of SiC/Al composites, with other parameters being constant, were controlled primarily by the intrinsic yield and tensile strengths of the matrix alloys. These figures also show that, in general, the yield and tensile strengths of the composites, with 20 vol % SiC_w reinforcement, were higher than those of the same heat-treated matrix alloys without reinforcement. The same trends of increased yield and tensile strengths were also observed for composites with these matrices with other forms of SiC reinforcements and other reinforcement contents.

Effect of reinforcement content.—The reinforcement content is another important factor controlling the strength of SiC/Al composites. The effect of the reinforcement content of a given type of SiC reinforcement, for a given matrix alloy, is shown in the 0.2-percent-offset yield strength histograms in figure 20(a) and the ultimate tensile strength histograms in figure 20(b). The results plotted are for specimens tested in the T6 temper, if applicable. The histograms show the highest and lowest strengths obtained from each type of composite. The average values from tests in the longitudinal and transverse orientations are also indicated by the "L" and "T" ticks on each bar.

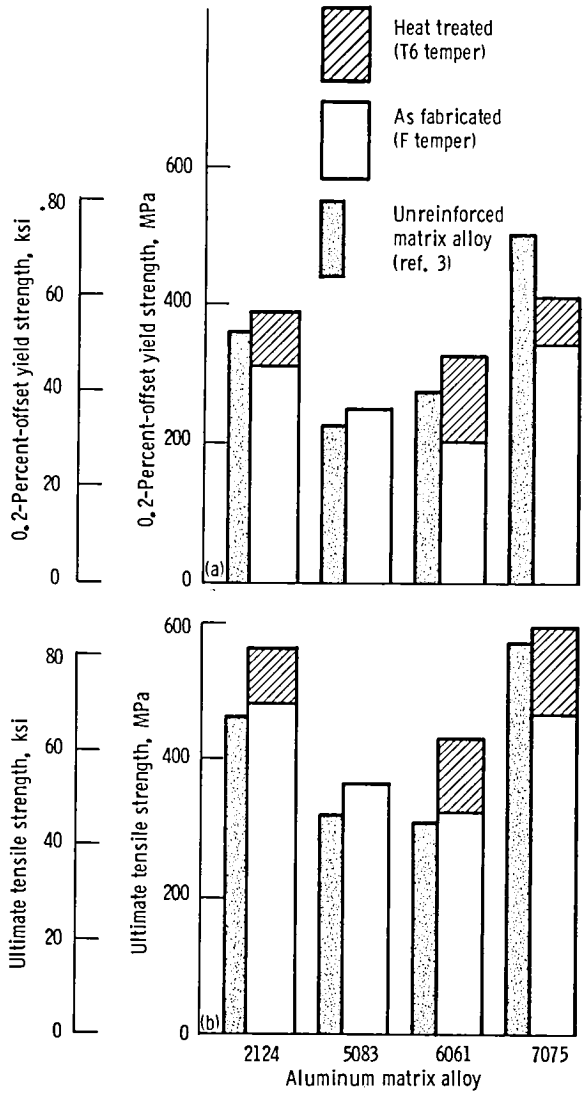

(a) 0.2-Percent-offset yield strength.
(b) Ultimate tensile strength.

Figure 19.—Effect of matrix alloy and heat treatment on strength of 20 vol % SiC_w-reinforced composites.

For a given matrix alloy and reinforcement the yield and tensile strengths generally increased with increasing reinforcement content. The yield strengths of the SiC/Al composites were increased by as much as 67 percent over those of the unreinforced matrix alloy; the ultimate tensile strengths were increased by as much as 56 percent. The increase in yield and tensile strengths was most dramatic for the 6061 and 5083 Al matrix composites.

The strength increase is partly explained by the stress-strain curves (fig. 9) for composites with each of the aluminum matrix alloys, tested in a given direction. These curves show that proportional limit stress, where the composite started into plastic flow, increased with increasing reinforcement content for each matrix alloy tested. The elastic modulus also increased with increasing reinforcement content and, although there did not seem to be a significant change in proportional limit strain, the stress-strain curves entered plastic flow at a higher flow stress. The slope of each stress-strain curve also increased as the composite entered plastic flow, and a higher flow stress was required to reach a given plastic strain until either a stable plastic flow was reached (ductile failure) or the specimen failed (brittle failure). This would indicate that the strength increase was caused by the closer packing of the reinforcement and the smaller interparticle spacing in the matrix. These caused increased interaction of dislocations with the SiC reinforcement, which resulted in increased work hardening, with higher flow stresses being required for the composite to reach a given strain.

The strength increased with increasing reinforcement content only as long as the composite was able to exhibit enough ductility to attain full strength. As the reinforcement content reached 30 to 40 vol % SiC, the rate of strength increase tended to taper off because the composites failed while still in the steeply ascending portion of the stress-strain curve. In this region the matrix probably did not have sufficient internal ductility to redistribute the very high localized internal stresses, and the composites failed before reaching stable plastic flow and normal ultimate strength. This was particularly true for the 5083 Al matrix composites. The failure strain fell to less than 1.5 percent at reinforcement contents of 20 vol %, and to less than 1 percent at 30 vol %. In these cases, stable plastic flow was never reached.

Effect of reinforcement type and directionality. – This investigation studied composites containing acicular SiC_w, irregular equiaxed nodular SiC_n, or irregular jagged SiC_p reinforcements. Stress-strain curves for 6061 Al matrix composites with 20 vol % of various SiC reinforcements indicated that the yield and ultimate tensile strengths were similar with SiC_w and SiC_p reinforcements but about 10 percent lower with SiC_n reinforcements. Composites with 30 vol % SiC_w and SiC_p reinforcements showed similar trends. No significant effect of directionality on strength properties was observed with 6061 Al matrix composites for any of the SiC reinforcements at contents from 10 to 40 vol % nor with 5083 Al matrix composites for reinforcement contents from 10 to 30 vol %.

Orientational differences were observed in composites with SiC_w reinforcement in 7075 and 2124 Al matrices. Stress-strain curves for these composites, with 20 vol % SiC_w reinforcement, showed that the ultimate tensile strengths of the heat-treated (T6 temper) composites were about 20 percent higher when tested in the transverse direction than in the longitudinal direction (fig. 21). SEM photographs of etched top surfaces of these composites (shown typically in fig. 22(a)) showed that they tended to have a more preferred whisker orientation than the

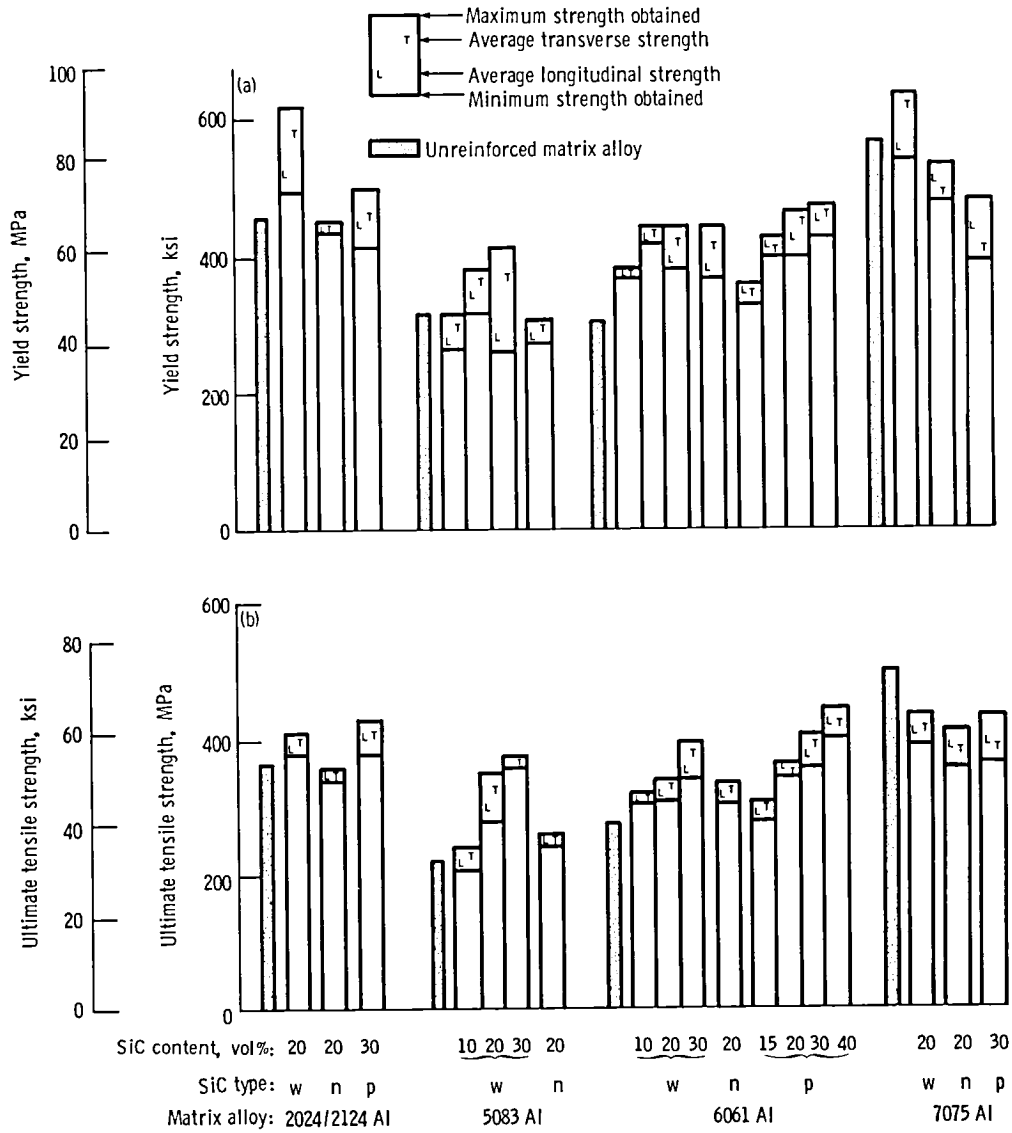

(a) 0.2-Percent-offset yield strength.
(b) Ultimate tensile strength.

Figure 20.—Effect of SiC reinforcement content and type on tensile properties of discontinuous SiC/Al composites. (SiC type: w denotes whisker; n denotes nodule; and p denotes particulate.)

6061 Al matrix composites (which had isotropic properties) presented in figure 4. This more preferred whisker orientation allowed the SiC whiskers to give an effective strength increase in the transverse direction.

The fracture surfaces of the 20 vol % SiC_w/7075 Al composites showed different fractures for specimens tested in the longitudinal and transverse directions. The 7075 Al matrix composite specimen (fig. 22(b)) had an ultimate tensile strength of 648 MPa (94.0 ksi) in the transverse direction but only 542 MPa (78.6 ksi) in the longitudinal direction. Many more whiskers projected out of the fracture surface of the composite transverse specimen than were observed for similar specimens tested in the longitudinal direction or in any of the 6061 Al composites (figs. 11 to 14). Similar trends were observed in the transverse fracture surfaces of the 20 vol % SiC_w/2124 Al composites (fig. 23), which also showed a 19 percent greater strength than specimens tested in the longitudinal direction. The whiskers were firmly embedded in the matrix and did not exhibit much

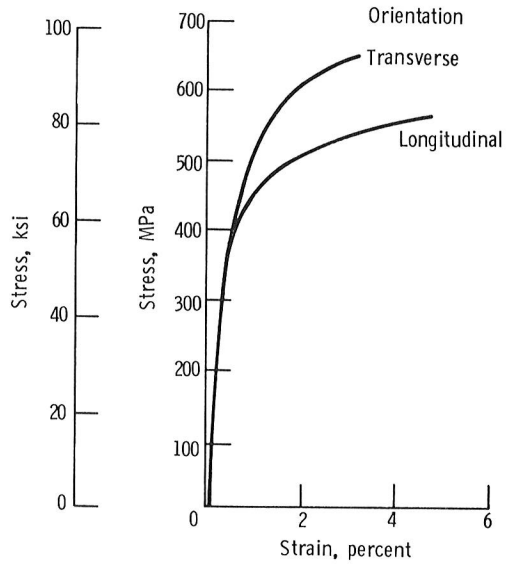

Figure 21.—Stress-strain curves of 20 vol % SiC_w/7075 Al composites tested in transverse and longitudinal orientations (T6 temper).

cratering at the whisker base. No matrix adhered to the exposed whiskers. Therefore the whiskers apparently merely pulled out of the matrix through interfacial shear. If shear pullout occurred, it would be improbable that the whiskers failed in tension, and the full length of the whisker (except for the one embedded end) is probably being viewed.

The yield strengths of these composites did not show a significant effect of orientation (fig. 20(a)). This again indicated that the SiC_w reinforcement did not significantly change the elastic modulus or the early plastic strain behavior of the composites. It only became effective at higher plastic strains, as increased dislocation interaction caused higher plastic flow stresses and thus higher tensile strength.

The general orientation of the SiC_w reinforcement in the transverse direction indicates that the whisker orientation was probably established during the initial extrusion phase of fabrication. The composites were then cross rolled normal to the extrusion direction, but the cross rolling did not appear to change the original whisker orientation. Thus the whisker alignment tended to be perpendicular to the final rolling direction. Throughout this study all orientations were based on the final rolling direction, so the orientation that is called the transverse direction in this study had a greater fraction of the SiC_w reinforcement aligned in that direction.

Where directional strengthening did occur with SiC_w reinforcement, a more preferred SiC_w orientation was present in the structure and the fracture surfaces

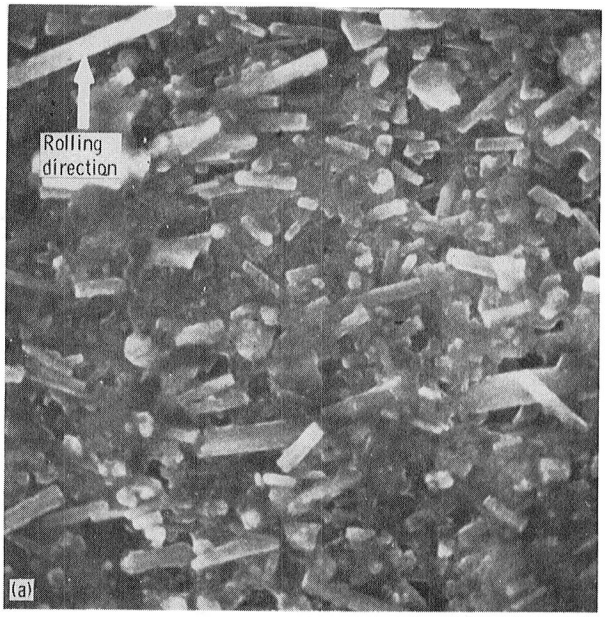

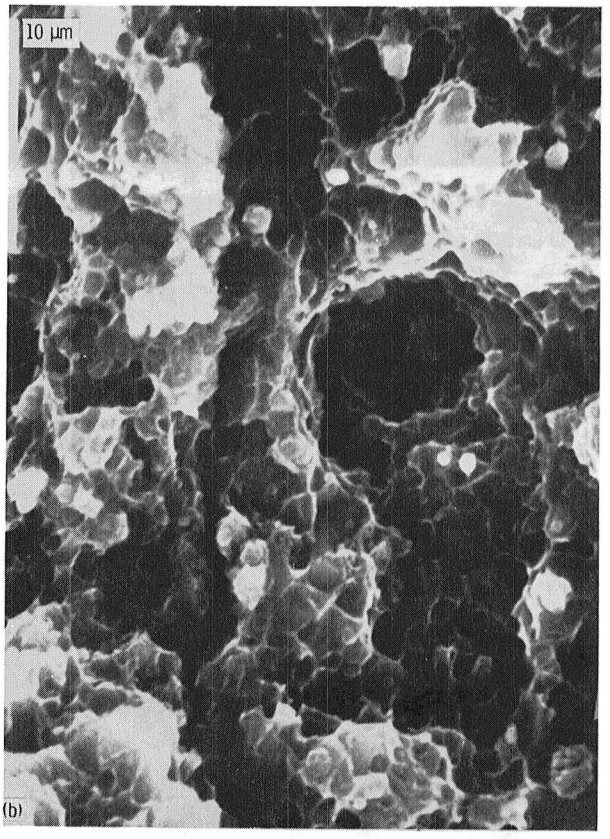

(a) General structure of etched top surface.
(b) Transverse orientation fracture edge.

Figure 22.—SEM photographs of 20 vol % SiC_w/7075 Al composite (T6 temper).

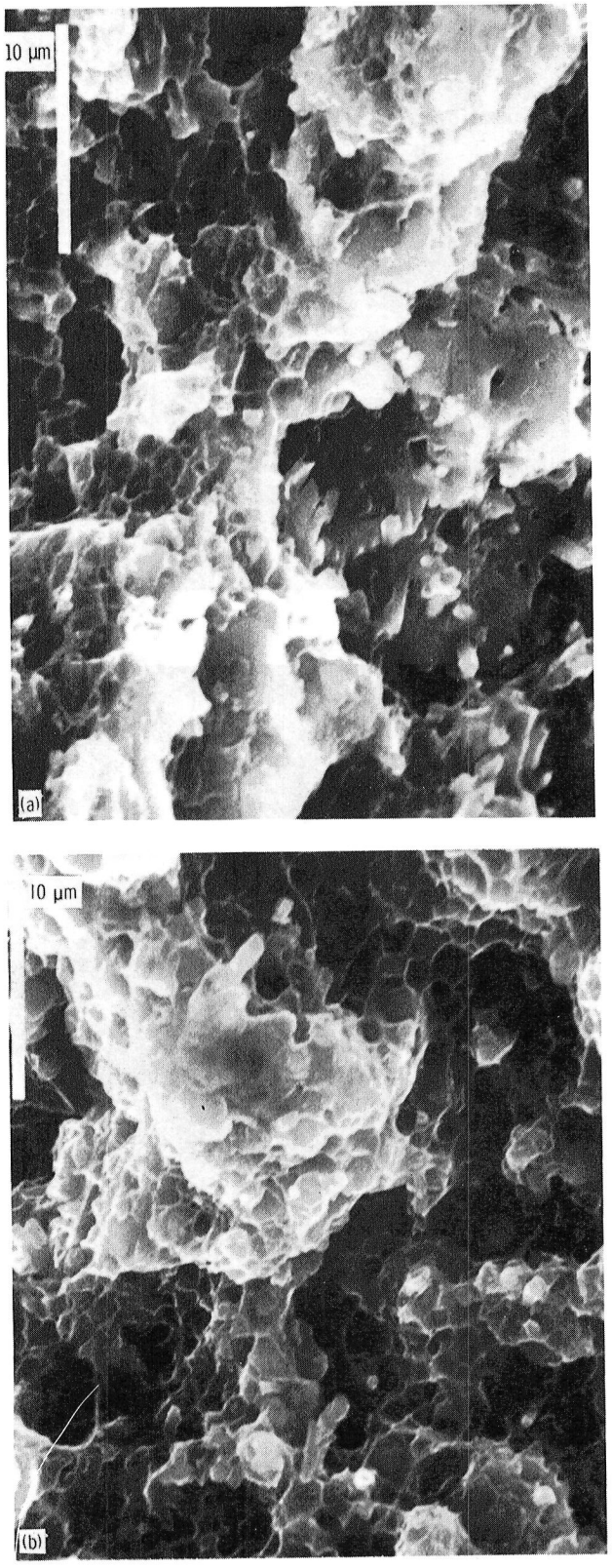

(a) Longitudinal orientation; failure strain, 3.4 percent; ultimate tensile strength, 500 MPa (72.5 ksi).
(b) Transverse orientation; failure strain, 4.3 percent; ultimate tensile strength, 596 MPa (86.4 ksi).

Figure 23.—SEM photographs of fracture surfaces of 20 vol % SiC_w/2124 Al composites (T6 temper).

indicated protruding whiskers (7075 and 2124 Al) with the whisker base still adherent to the matrix and no crater at the base. Where no directionality was observed (6061 and 5083 Al), the reinforcement was more randomly oriented and the fracture surfaces showed that the matrix pulled away from the whisker and formed a crater. This may have fractured the whisker but more probably established a fracture path through the matrix just beyond the ends of the whiskers. In both situations, however, no matrix adhered to the surfaces of the projecting whiskers. Thus the full-strength properties of the whiskers were probably never attained, and failure occurred by whisker/matrix interfacial shear pullout.

All the composites with SiC_w reinforcement tested in the longitudinal direction, regardless of the aluminum matrix, had tensile strengths fairly comparable to those of composites with the nearly equiaxed SiC_p and SiC_n reinforcements. Although some strength increases were observed in the direction of the reinforcement orientation for the SiC_w/Al composites, the effect was not universal and should be considered further. Since the modulus and the yield and tensile strengths for the SiC_w/Al composites were comparable to those of the SiC_n and SiC_p composites in all cases in the direction perpendicular to the SiC_w reinforcement, and in some cases parallel to the reinforcement, at the current state of the art, the reinforcing process in these composites appears to be more of a dispersoid strengthener than a fiber strengthener.

Further process development to increase the SiC whisker length and to promote better fabrication may allow a greater amount of the potentially high properties of the SiC_w reinforcement to be utilized. The maximum aspect (length/diameter) ratio observed for these whiskers was about 38. However, this value is probably somewhat low because of foreshortening in the photographs and submerged embedment of the ends in the remaining matrix, but the actual value is probably less than the average aspect ratio of 75 reported for as-produced whiskers in reference 4.

With further development the SiC_w/Al composites may prove more advantageous for specialized applications. For whisker reinforcement to be effective, assuming adequate whisker/matrix bonding, three factors must be considered: whisker surface perfection, sufficient whisker length, and whisker orientation. The whiskers must be preferentially oriented within a few degrees of the loading axis, and the whisker surface must remain perfect. The fabrication processes used to produce SiC_w/Al composites inherently set up conditions that work against effective utilization of full whisker properties in these composites. First, in the reinforcement/powder blending process, it is highly probable that the whisker surfaces will become flawed and that their intrinsic, as-produced strength and aspect ratio will be reduced. Second, the extrusion of the

sintered SiC/Al billets will further break up the whiskers and further flaw their surfaces. In addition, conventional extrusion can, at best, only partially orient the SiC_w reinforcement. The SEM distribution photographs show a general orientation in the extrusion direction, but it is nowhere near the $\pm 5°$ to $\pm 10°$ required for optimum reinforcement.

With the current state of the art of SiC reinforcement production and composite fabrication, it may be more beneficial to treat all SiC/Al composites, regardless of reinforcement type, as a single class of isotropic materials and to use their commonality with conventional aluminum alloys as a major advantage. Thus established aluminum component design and conventional aluminum metalworking and forming processes could be used. The main advantage of discontinuous SiC/Al composites is their similarity to conventional aluminum alloys and their relative isotropy of properties. Promoting anisotropy of properties by using more delicate blending and orientation processing would present difficulties to the final user. Severe anisotropy of properties can make the final application of these composites more difficult and more expensive. If highly oriented whiskers were to be used, the orientation would have to be constantly monitored to avoid misalignment during component assembly by the end user. Thus fabrication costs to the user would be increased as the required processing would start to approach that of conventional fiber layup composite fabrication. In addition, component design would be more complex. Anisotropy in strength would probably require designers to use only the lower strength orientation as the design strength value.

Because of the limitations of currently available SiC_w reinforcements and of fabrication methods currently being used, it is debatable if SiC_w reinforcements offer a significant advantage over SiC_n and SiC_p reinforcements at this time. However, as whisker reinforcement production and composite fabrication technologies evolve, the SiC_w reinforcement may ultimately allow a considerable increase in composite strength. The final choice of reinforcement type would probably evolve into a user decision based on the cost and availability of desired structural shapes from the fabricator.

Factors Influencing Ductility of Discontinuous SiC/Al Composites

The ductility, as measured by strain to failure, of the SiC/Al composites, is again a complex interaction of parameters. However, the primary factors affecting the properties are reinforcement content, matrix alloy, and orientation.

With increasing reinforcement content the failure strain of the composites is reduced and the stress-strain curves also reflect a change in the fracture mode. Failure strains for the various composites tested are plotted in figure 24(a) as a function of SiC reinforcement content for 6061 Al matrix composites in both the F and T6 tempers. Figures 24(b) to (d) show similar plots for the other aluminum matrix alloys tested in the optimized temper for each alloy. The different types of fracture modes observed are presented in figure 25. SEM photographs of typical fracture surfaces for each of these failure modes are shown in figures 11 to 14.

In general, the ductility behavior of the composites was independent of the type of SiC reinforcement used. The SiC_w composites failed by a slightly different mechanism than did the SiC_p and SiC_n composites, as shown schematically in figure 26. SEM photographs of the fracture surfaces of the transverse SiC_w/Al composites show that the fracture occurred with the formation of a small crater around the embedded base of the whisker, an attendant small area of matrix being restrained by the reinforcement. Because of the small diameter of the SiC_w reinforcement, these craters were small and allowed a greater area of unrestrained matrix to fail in fine, lacy dimple networks. Fracture occurred in longitudinal SiC_w/Al composites because of the larger areas of ductile, fine dimple networks in the matrix, as fewer SiC whiskers were oriented to restrain the matrix. The SiC_p and SiC_n reinforcements caused a much larger diameter crater, approximating the diameter of the reinforcement. This behavior indicated that the fracture path went along the edges of adjacent SiC particles. It could not be determined if fracture occurred at the reinforcement/matrix interface or in the matrix in close proximity to the edges of the reinforcement. These large craters decreased the area of unconstrained matrix and limited the amount of matrix available for ductile, dimpled fracture. However, because of the greater number of smaller diameter SiC whiskers required to give an equivalent reinforcement content, the effects of this constrained matrix volume tended to balance out and the failure strains of the composites tended to be similar, regardless of the type of SiC reinforcement used.

Preliminary tensile tests were conducted on wrought aluminum specimens with no SiC reinforcement. These specimens exhibited failure strains of about 15 percent, with a smooth 45° chisel-point shear fracture across the thickness of the specimen. There was also a contraction in the width of the specimen at the fracture plane.

Composite specimens with low reinforcement contents of 10 to 20 vol % SiC in 6061 Al exhibited the same type of smooth 45° chisel-point shear fracture across the thickness but without the width contraction (fig. 25). Failure strains of 6 to 12 percent were observed with this type of fracture. SEM photographs of 10 vol % SiC_w/6061 Al and 15 vol % SiC_p/6061 Al composites showed a ductile fracture with a fine, lacy dimple network (fig. 11).

The failure strain of these low-reinforcement-content composites was influenced by orientation (fig. 27). The 10 vol % SiC_w/6061 Al composites showed a somewhat

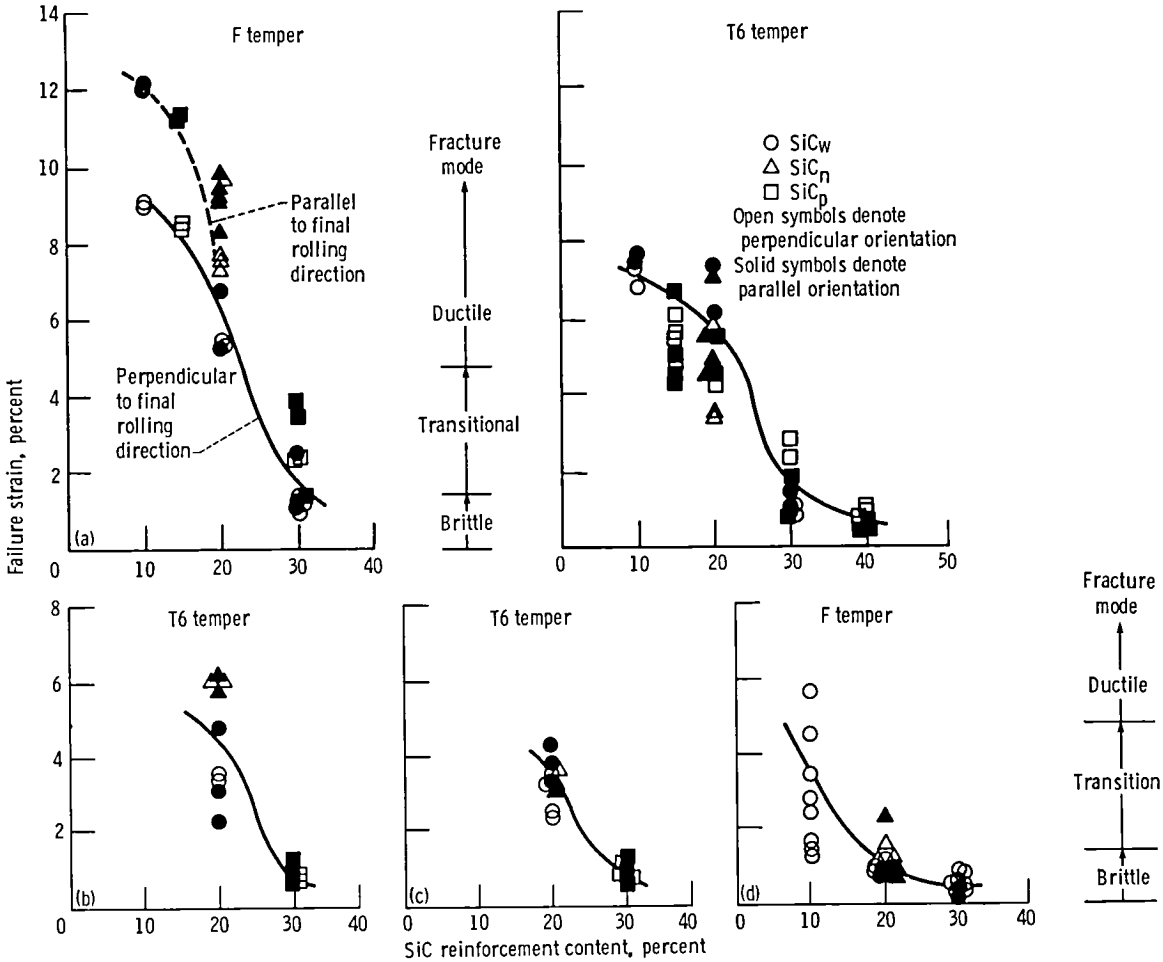

(a) 6061 Al matrix.
(b) 7075 Al matrix.
(c) 2024/2124 Al matrix.
(d) 5083 Al matrix.

Figure 24.—Failure strain of SiC/Al composites.

preferred orientation of whiskers parallel to the transverse direction. A similar, but smaller, orientation effect on ductility was also observed in the 10 vol % SiC_w/5083 Al composites. The 15 vol % SiC_p/6061 Al composites showed a working texture and reinforcement stratification parallel to the transverse direction. Each of these composites had higher failure strains in the longitudinal direction than in the transverse direction. The differences were only observed for composites tested in the as-fabricated (F temper) condition. This orientation effect on ductility disappeared for both composites after heat treatment. Thus the orientation effect is probably due to working texture from extrusion or rolling rather than to reinforcement orientation effects since any texture arising from mechanical working would probably be eliminated by recrystallization during solution heat treatment. In addition, this directional effect on ductility was observed for the randomly oriented SiC_p/Al composites as well as for the generally oriented SiC_w/Al composites. This again points to a working texture effect rather than a composite reinforcement effect.

Composites with lower reinforcement contents also showed a difference in dimple structure at the fracture surface with different orientations. The fracture surfaces in the more ductile orientations showed a fine dimple network structure; in the less ductile direction the dimple network structures were slightly coarser (fig. 11).

No significant effects of orientation on failure strain were observed with any of the matrix alloys containing 20 vol % or greater SiC reinforcement. No SiC_w orientation effects on ductility in 7075 and 2124 Al matrix composites were evidenced by the similar failure strains of these composites, regardless of testing direction. However, no composites with reinforcement contents of less than 20 vol % were tested for these alloys.

At intermediate reinforcement contents (20 vol %) the failure strain was reduced to the 5 to 2 percent range, and the fracture behavior underwent a transition. At the

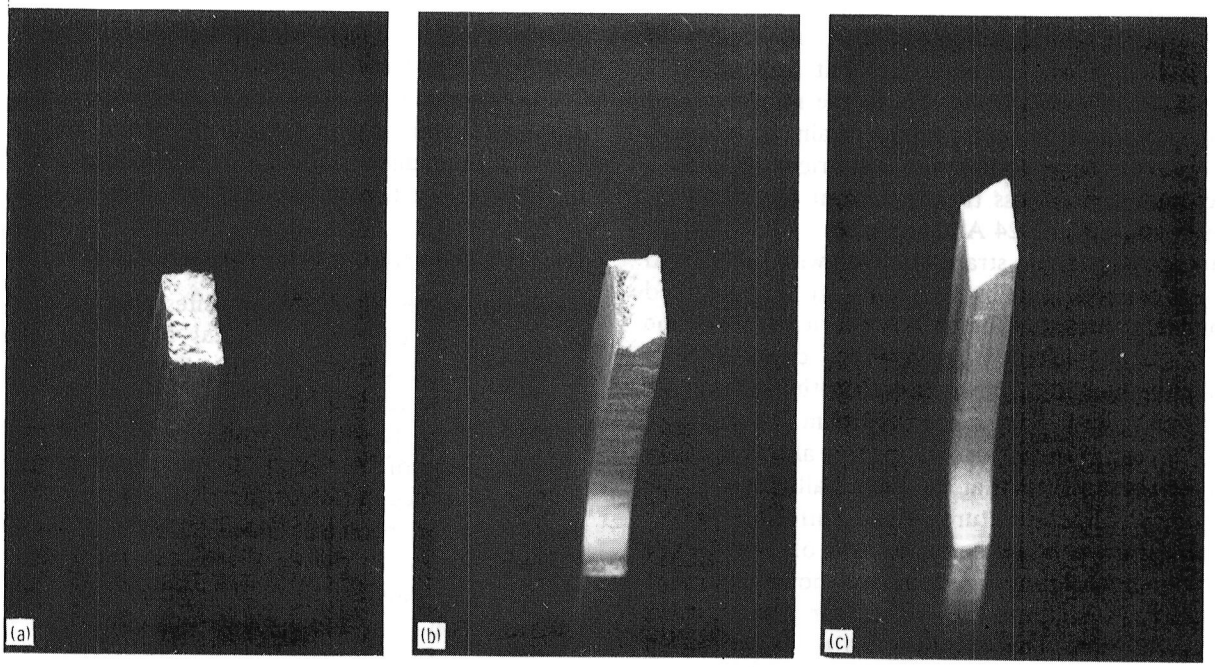

(a) Brittle (flat); failure strain, 0 to 2 percent.
(b) Transition (transitional); failure strain, 2 to 5 percent.
(c) Ductile (chisel point); failure strain, greater than 5 percent.

Figure 25.—Fracture modes of SiC/Al composites.

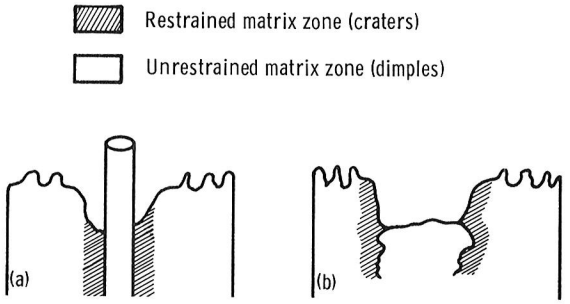

(a) SiC_w reinforcement.
(b) SiC_n and SiC_p reinforcement.

Figure 26.—Schematic sketch of cratering size effect observed from SEM of fracture surfaces.

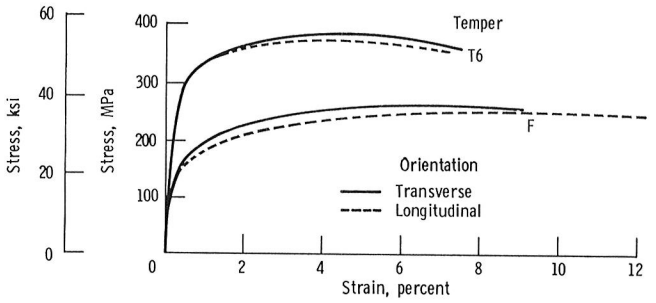

Figure 27.—Stress-strain curves of 10 vol % SiC_w/6061 Al composites tested in longitudinal and transverse orientations.

higher strain portion of this range a 45° shear lip formed at each side of the width of the fracture and the lips intersected to form a "V" (fig. 25). The fracture surfaces of composites in this intermediate reinforcement range show a coarsening of the dimple network (fig. 12). At the lower strain portion of this range a smooth 45° chisel formed at one edge, extended about half-way through the width of the specimen, and then became flat and granular for the remainder of the section thickness. Figure 13 shows the transition zone where the shear lip intersected with the flat plane. The coarsened dimple area and the cleavage are evident.

At reinforcement contents of 30 and 40 vol % the fracture became flat and granular across the entire width, with no evidence of a chisel-point shear lip (fig. 25). Composites exhibiting this type of fracture mode failed in a brittle manner, with a failure strain of 2 percent or less. SEM photographs of this type of fracture showed cleavage fractures with some coarse dimple networks still visible (fig. 14). As the reinforcement content increased, the ductility decreased and a higher percentage of the fracture surface area failed by cleavage. The most brittle composites failed with a granular fracture surface.

Previous results reported for SiC/Al composites tended to show lower failure strains than were observed in the current study. Reference 6 reports failure strains of 1 to 2 percent for SiC_w/6061 Al composites and shows slightly higher failure strains for composites with SiC_n reinforcement. Reference 9 reports failure strains of less than 1 percent for 15 vol % SiC_w in 2024 and 6061 Al

matrices. Reference 10 reports failure strains of about 4.5 percent parallel to the direction of SiC_w reinforcement in 20 vol % SiC_w/6061 Al composites but only about 2 percent in the direction transverse to the reinforcement direction. Reference 5 reports failure strains of less than 2.5 percent for several aluminum matrices with SiC_p reinforcement and of less than 1 percent for 20 vol % SiC_w/2024 and SiC_n/2024 Al composites.

The increase in failure strain observed with the SiC/Al composites tested in this investigation can be attributed to two main factors. First, the fabricators of the composites are constantly striving for cleaner, more uniform aluminum alloy powders with optimized powder compositions and for more uniform control of fabrication variables. Cleaner, purer alloy powders contain fewer impurities that can potentially form brittle intermetallics in the structure. More uniform powders and reinforcements allow better control of powder size distribution, interparticle spacing, and homogeneity of the structure. In addition, the evolutionary development of the composites also includes better beneficiation processing to separate out debris and unwanted particles from the reinforcement. Thus when comparing data reported for these SiC/Al composites, the date that the composites were fabricated becomes important, since this helps to define the fabrication state of the art of the composites, which in turn helps to determine the state of evolution of the strength and ductility behavior.

The second factor affecting the improvement of the ductility of the SiC/Al composites studied in this investigation is that these composites were more heavily worked than most of the composites previously reported. NASA Lewis chose to have larger lots of material delivered, so 15.2-cm (6-in.) diameter and 15.2-cm (6-in.) long billets of SiC_w- and SiC_n-reinforced aluminum matrix composites were prepared by ARCO Metals. These billets were extruded and then rolled to 2.54-mm (0.100-in.) thick plates. This processing gave a maximum reduction in area by extrusion of 91.2 percent, which was followed by a further 75 percent reduction in area by rolling, for a total maximum reduction in area of 97.9 percent by working. Similar processing of smaller, 7.6-cm (3-in.) diameter, billets would give only a 91.5 percent maximum reduction in area. Although these reductions are maximums, they do give an indication of the amount of mechanical work that has been put into the composites. The actual reductions would be smaller because of billet porosity, cropping, and scrappage. The composites made by DWA were also heavily worked during fabrication.

Increased reduction by mechanical working helps to increase composite ductility in three ways: it reduces matrix porosity to a greater degree, it breaks up inclusions and more effectively stringers them, and it makes the dispersion of matrix and reinforcing particles finer and more uniform. All three factors would have a beneficial effect on composite ductility. The SEM study showed that the particles of the SiC_p and SiC_n reinforcements were very much coarser than those of the SiC_w reinforcement. The effects of the finer particle sizes of the SiC_p and SiC_n reinforcements should be studied to see if a finer dispersion of these reinforcements could further increase the strength and ductility.

Elevated-Temperature Properties of SiC/Al Composites

Discontinuous SiC/Al composites continued to show an advantage over conventional aluminum alloys at elevated temperatures (fig. 10). The load-time curves show the same general behavior at temperatures of 149° to 204° C (300° to 400° F), with the specimens exhibiting the same type of V-shaped, double shear lip transition fracture observed in tests at room temperature. The load-time curves for specimens tested at 260° C (500° F) show a slight increase in plastic strain, but the fracture was basically the same as that observed in the other tests. Although still transitional, the fracture showed a greater tendency to form a more ductile, single shear lip. The load-time failure strain appeared to increase slightly at 316° C (600° F), but the fracture behavior changed markedly. The fracture showed a great deal of necking in both the width and thickness directions of the specimen, and all four surfaces of the fracture area necked in a ductile manner (fig. 28). This change in fracture behavior coincided with the marked drop in ultimate tensile strength observed at this temperature.

Reference 11 reports that 20 vol % SiC_w/2024 Al composites showed a similar strength advantage at elevated temperatures over unreinforced 2024 Al. In that work, round tensile test specimens were used and reduction-in-area measurements could be made at the necked fracture area. At temperatures of less than 240° C (460° F) the composites failed with relatively little plastic flow and no necking. At 240° C (460° F) the composites showed an abrupt change in behavior, exhibited significant necking, and failed at plastic strains of about 10 percent. Further tests at temperatures to about 400° C (752° F) showed similar behavior, with the plastic strain increasing to about 11 percent.

The results obtained in this investigation (fig. 10), as well as those results reported in reference 11, show that SiC/Al composites offer about a 109 deg C (200 deg F) increase in use temperature over conventional aluminum alloys. The results also indicate that SiC/Al composites have the potential to be used effectively at temperatures to at least about 204° C (400° F).

Comparison of Properties of Discontinuous SiC/Al Composites with Al-Li-Mg Alloys

The discontinuous SiC/Al composites studied in this investigation demonstrated very good modulus and modulus/density improvements, and some strength

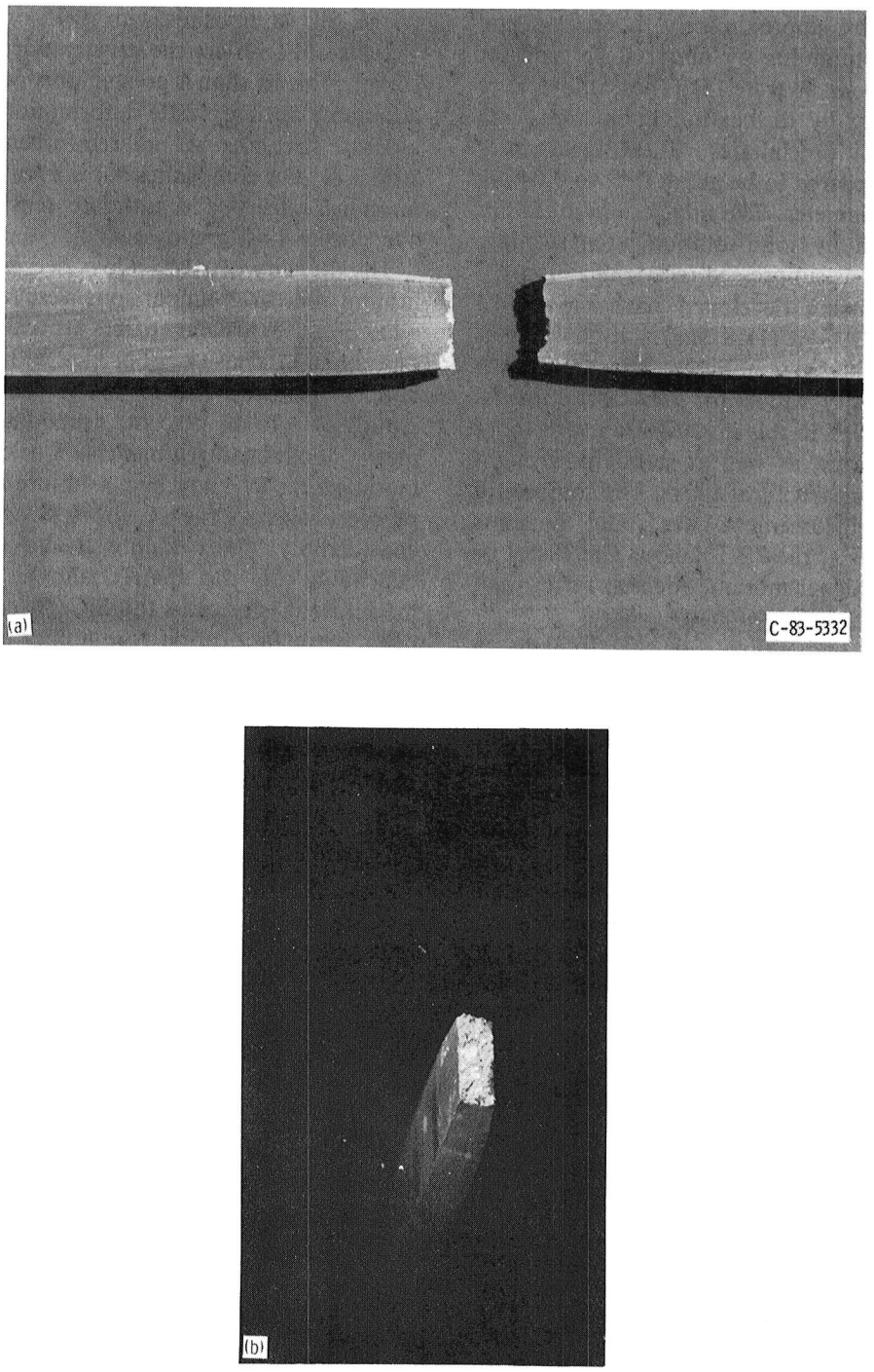

(a) Failed specimen after tensile testing.
(b) Fracture surface.

Figure 28.—Failed 20 vol % SiC_w/6061 Al composite specimens after tensile testing at 316° C (600° F).

improvement, over standard wrought aluminum alloys. However, their properties should also be compared with those of a new class of Al-Li alloys that are becoming commercially available from Alcoa under the trade name Alithalite (ref. 12). Although still not commercially available, these new alloys will be based on those developed in the research described in references 13 and 14. These Al-Li alloys contain about 1 to 3 wt % lithium, 2 to 5 wt % magnesium, and 0.3 wt % manganese. Of this class, the 2.3Li-3.5Mg alloy will probably give the best combination of modulus, density, and ductility. The moduli of these alloys increased, while the ductility and density decreased, with increasing lithium content. Each weight percent of lithium added to an aluminum alloy

reduced its density by approximately 3 percent and increased the elastic modulus by about 6 percent for lithium additions to 4 wt % (ref. 15). These alloys were strengthened primarily by dislocation interaction with fine metastable Al_3Li precipitates. These precipitates were spherical and appeared to be about 0.02 to 0.04 μm (0.80 to 1.6 μm) in diameter. The magnesium additions increased the strength by solid-solution strengthening; the manganese additions suppressed recrystallization.

The Al-Li alloys being developed have moduli of elasticity as high as 81 GPa (11.8 Msi) and densities as low as 2.45 g/cm^3 (0.089 lb/in^3). Figure 29 compares the relative modulus/density ratios for the discontinuous Si/Al composites studied in this investigation with those of three Al-Li-Mg alloys, as well as standard wrought aluminum and titanium structural alloys. The composites with 15 vol % SiC reinforcement have about the same modulus/density ratios as the 2.3 Li alloy. The 20 vol % SiC composites have higher modulus/density ratios than any of the Al-Li alloys.

The ratios of yield and ultimate tensile strengths to density for the various aluminum-base materials are compared in figure 30. The lower end of each hatched section represents the 0.2-percent-offset yield strength/density value; the top end represents the ultimate tensile strength/density value. The failure strain of each material is shown at the base of the bar. This plot shows that the yield strength/density ratio of the Al-2.3Li-3.5Mg alloy (refs. 13 and 14) is higher than those for any of the composites, but the ultimate tensile strength/density ratio is lower than those for the 20 vol % SiC composites with 7075 or 2024 Al matrices. These results reflect the greater ductility of the SiC/Al composites, in that a greater portion of the strength is attainable during plastic deformation between yield and ultimate strengths. At SiC reinforcement contents above 20 vol %, the composites show even greater increases in modulus/density and ultimate tensile strength/density over the Al-Li-Mg alloys.

The ductility of Al-Li alloys decreased with increasing lithium content. Comparisons were made with the 2.3 Li alloy because this alloy offers attractive modulus/density and strength/density properties with a failure strain of about 4 percent. The 15 vol % composites had failure strains of 4 to 12 percent, depending on the aluminum matrix alloy, heat treatment, and orientation. The higher modulus 3.1 Li alloy had a failure strain of about 1.5 percent, whereas the 20 vol % SiC/Al composites had considerably higher failure strains (2.9 to 5.6 percent depending on the matrix alloy). Thus for a given modulus/density ratio the SiC/Al composites probably offer more fabrication formability and service ductility than the Al-Li-Mg alloy class.

Application of SiC/Al Composites to Aircraft Engine and Aerospace Structures

The results of this study show that low-cost SiC/Al matrix composites, currently projected to sell for about \$9/kg (\$20/lb), demonstrate a good potential for application to aerospace structures and aircraft engine components. These composites merit additional work to

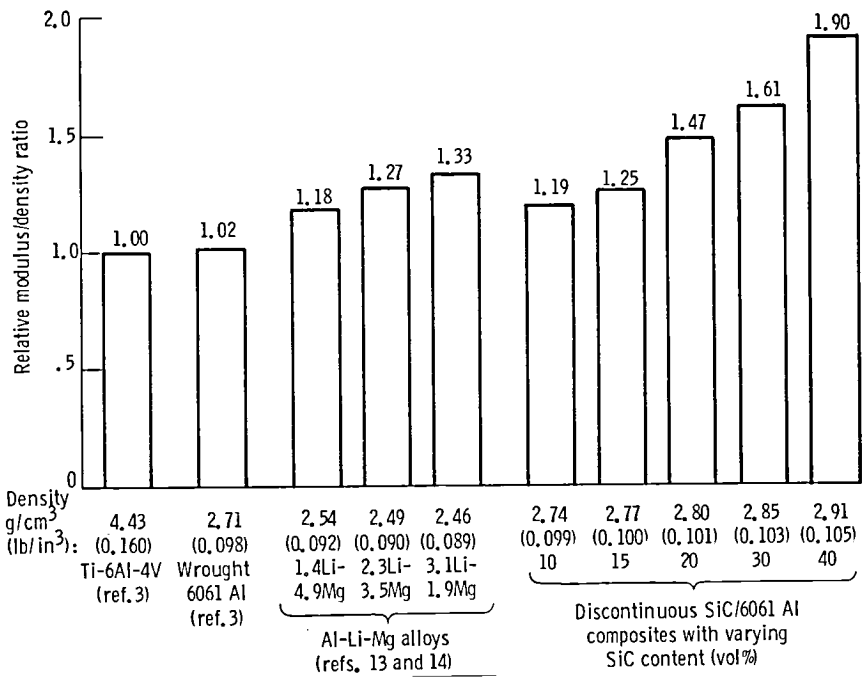

Figure 29.—Modulus/density ratios of discontinuous SiC/Al composites with aluminum, titanium, and Al-Li-Mg alloys.

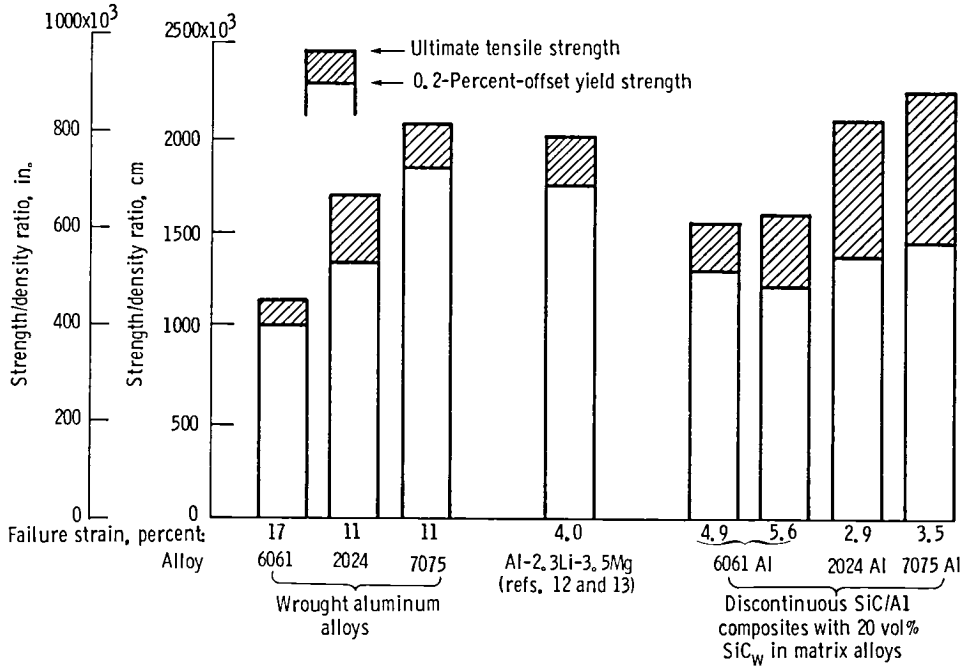

Figure 30.—Yield strength/density and ultimate tensile strength/density ratios of aluminum-base materials.

determine their fatigue, long-term stability, and thermal cycle behavior in order to more fully characterize their properties and allow their consideration for structural design in a variety of aircraft and spacecraft applications. The composites are formable with normal aluminum metalworking techniques and equipment at warm working temperatures, and they can be made directly into structural shapes during fabrication with a minimum of final machining required. This use of conventional forming equipment with minimum additional part finishing required could further reduce the component costs to the user.

The most significant aspect of these data is the increase in modulus over those of competitive aluminum alloys. Figure 29 compares the relative modulus/density ratios of various structural alloys with the composites tested in this study. Again, the moduli of the composites are basically dependent only on the reinforcement content and are independent of reinforcement type and matrix alloy. These results show that at 20 vol % reinforcement the moduli of elasticity of SiC/Al composites can be increased about 50 percent above that of aluminum, to a value approaching that of titanium. This increase in modulus is achieved with a material having a density one-third less than that of titanium. At 30 vol % SiC the advantage was increased to about 70 percent; at 40 vol % SiC the modulus was almost double that of unreinforced aluminum alloys and almost twice the modulus/density ratio of conventional aluminum and titanium structural alloys.

The Boeing Company has reported that it expects to save about 10 percent of the structural weight of advanced transports currently under design by using new Al-Li (ref. 16). The modulus/density advantages shown in this current study of SiC/Al composites offer better modulus, modulus/density, and ductility properties than do the Al-Li alloys. The SiC/Al composites have about the same yield and ultimate tensile strengths, and so using these SiC/Al composites could save appreciably more weight in airframe and engine structures and could reduce aircraft weight by possibly as much as twice that projected when using the Al-Li alloys.

For applications where a material with a high modulus (in the range 103 GPa (15 Msi)), high strength, and good ductility are required, a 20 vol % SiC/Al composite could be substituted. These composites, with a 6061 Al matrix, would give reasonable yield and tensile strengths with high strain to failure and probably good fracture toughness to offer a reasonable margin of safety under operating conditions. If higher strengths are desired while retaining high ductility, a 20 vol % SiC_n/7075 Al composite could be used. If still higher strengths are required, and ductility is not as critical, 20 vol % SiC_w/7075 Al or 2124 Al composites could be used. For applications where maximum stiffness is required, a 30 vol % SiC composite with 6061 Al matrix could be used to gain stiffness (modulus of 124 GPa (18 Msi)) while retaining high strength and reasonable ductility. If maximum modulus (124 to 152 GPa (18 to 22 Msi)) and ultimate tensile strength (621 MPa (90 ksi)) are required,

a 30 to 40 vol % SiC composite with a 2024/2124 Al or 7075 Al matrix would have excellent potential.

Conclusions

Studies were undertaken to assess the potential of applying low-cost discontinuous SiC/Al composites to aircraft engine components and structures. Panels were fabricated with SiC whisker, nodule, or particulate reinforcements and delivered to the NASA Lewis Research Center for evaluation. Tensile tests were conducted on the SiC/Al composites, and the effects of reinforcement type, matrix alloy, reinforcement content, and orientation were determined by analysis of stress-strain curves and by SEM examination of the structures of the composites. This investigation led to the following conclusions:

1. The discontinuous SiC/Al composites offer a 50 to 100 percent increase over the modulus of unreinforced aluminum and offer a modulus equivalent to that of titanium, but at a third less density. The SiC/Al composites have modulus/density ratios almost twice those of titanium alloys. The moduli of SiC/Al composites tend to be isotropic and are controlled by the amount of SiC reinforcement.

2. The yield and ultimate tensile strengths of the SiC/Al composites were up to 60 percent greater than those of the unreinforced matrix alloys. The yield and ultimate tensile strengths of the composites were controlled primarily by the type and temper of the matrix alloy and by the reinforcement content. In general, however, these properties were independent of the type of reinforcement used. This suggests that with the present state of the art of materials and fabrication, SiC particulate and nodule reinforcements are as effective as whisker reinforcement.

3. The ductility, as measured by strain to failure, of the SiC/Al composites was dependent on the reinforcement content and the matrix alloy. Composites with ductile matrix alloys and lower reinforcement contents exhibited a ductile shear fracture with a 5 to 12 percent failure strain. As reinforcement content increased, the fracture progressed through a transition and became brittle, reaching a less than 1 to 2 percent failure strain, at higher reinforcement contents.

4. A fine dimple network was observed in the fracture surfaces of composites with higher fracture strains. At lower fracture strains a coarser dimple network was observed. Composites failing in a brittle manner showed increasing amounts of cleavage fracture. As-fabricated SiC/Al composites tended to be more ductile in the direction perpendicular to initial extrusion. With subsequent heat treatment, and at higher reinforcement contents, the failure strains tended to become isotropic and independent of orientation.

5. The SiC whisker reinforcement was generally oriented in the extrusion direction. Composites with a higher degree of preferred orientation tended to show higher ultimate tensile strengths in the direction of whisker orientation. Composites with more random whisker orientations tended to be isotropic in strength.

6. Comparison of properties with aluminum structural alloys and with Al-Li alloys showed that low-cost, lightweight aluminum matrix composites containing discontinuous SiC reinforcement demonstrated very good potential for application to aircraft engine components and aerospace structures.

Lewis Research Center
National Aeronautics and Space Administration
Cleveland, Ohio, February 1, 1984

References

1. McDanels, D. L.: A Review of NASA Research on Impact-Resistant Boron/Aluminum Composites. NASA TM-83391, 1983.
2. McDanels, D. L.; and Signorelli, R. A.: Evaluation of Low-Cost Aluminum Composites for Aircraft Engine Structural Applications. NASA TM-83357, 1983.
3. Metals Handbook. Vol. 1. Eighth ed., American Society for Metals, 1961.
4. Bechtold, B. C.; Beatty, R. L.; and Cook, J. L.: Silicon Carbide Whiskers from Rice Hulls—A Unique Reinforcement. Progress in Science and Engineering of Composites, Vol. 1, T. Hayshi, K. Kawata, and S. Umekawa, eds., Japan Society for Composite Materials, 1982, pp. 113-120.
5. Harrigan, W. C., Jr.; Nowitzky, A. M.; and Supan, E. C.: Production and Characterization of Advanced Particulate-Reinforced Powder Metallurgy Products. DWA-600, DWA Composite Specialties, Inc., 1982.
6. Rack, H. J.; Baruch, T. R.; and Cook, J. L.: Mechanical Behavior of Silicon Carbide Whisker Reinforced Aluminum Alloys. Progress in Science and Engineering of Composites, Vol. 2, T. Hayshi, K. Kawata, and S. Umekawa, eds., Japan Society for Composite Materials, 1982, pp. 1465-1472.
7. Gomes de Mesquita, A. H.: Refinement of the Crystal Structure of SiC Type 6H. Acta Crystalligr., vol. 23, 1967, pp. 610-617.
8. Rochow, E. G.: Silicon. Comprehensive Inorganic Chemistry, J. C. Bailar et al., eds., vol. 1, Pergamon Press, 1973, p. 1421.
9. Divecha, A. P.; Fishman, S. G.; and Karmarkar, S. D.: Silicon Carbide Reinforced Aluminum—A Formable Composite. J. Met., vol. 33, Sept. 1981, pp. 12-17.
10. Nieh, T. G.; and Karlak, R. F.: Hot-Rolled Silicon Carbide-Aluminum Composites. J. Mater. Sci. Lett., vol. 2, no. 3, Mar. 1983, pp. 119-122.
11. Phillips, W. L.: Elevated Temperature Properties of SiC Whisker Reinforced Aluminum. ICCM/2, Proceedings of the Second International Conference on Composite Materials, B. R. Noton, et al. eds., Metallurgical Society of AIME, pp. 567-576.
12. ALCOA R&D Report: Aerospace Materials Technology. Aviat. Week Space Technol., vol. 119, no. 13, Sept. 26, 1983, pp. 108-109.
13. Sanders, T. H., Jr.: Development of an Al-Mg-Li Alloy—Corrosion Resistance. NADC-76397-30, Aluminum Co. of America, 1976. (AD-A034954.)

14. Starke, E. A., Jr.; Sanders, T. H., Jr.; and Palmer, I. G.: New Approaches to Alloy Development in the Al-Li System. J. Met., vol. 33, no. 8, Aug. 1981, pp. 24-33.
15. Sankaran, K. K.; and Grant, N. J.: Structure and Properties of Splat Quenched 2024 Aluminum Alloy Containing Lithium Additions. Aluminum-Lithium Alloys, T. H. Sanders, Jr., and E. A. Starke, Jr., eds., Metallurgical Society of AIME, 1981, pp. 205-227.
16. Airframe Makers Review Options. Aviat. Week Space Technol., vol. 118, no. 23, June 6, 1983, pp. 29-32.

1. Report No.	2. Government Accession No.	3. Recipient's Catalog No.
NASA TP-2302		

4. Title and Subtitle	5. Report Date
Microstructure and Orientation Effects on Properties of Discontinuous Silicon Carbide/Aluminum Composites	July 1984
	6. Performing Organization Code: 505-33-32

7. Author(s)	8. Performing Organization Report No.
David L. McDanels and Charles A. Hoffman	E-1977
	10. Work Unit No.

9. Performing Organization Name and Address	11. Contract or Grant No.
National Aeronautics and Space Administration Lewis Research Center Cleveland, Ohio 44135	
	13. Type of Report and Period Covered: Technical Paper

12. Sponsoring Agency Name and Address	14. Sponsoring Agency Code
National Aeronautics and Space Administration Washington, D.C. 20546	

15. Supplementary Notes

16. Abstract

Composite panels containing up to 40 vol % discontinuous SiC whisker, nodule, or particulate reinforcement in several aluminum matrices were commercially fabricated and delivered to NASA Lewis for evaluation of mechanical properties and microstructural characteristics. The elastic modulus of the composites was found to be isotropic and independent of the type of reinforcement used and was controlled solely by the volume percentage of SiC reinforcement present. The yield and tensile strengths and the ductility were controlled primarily by the matrix alloy, the temper condition, and the reinforcement content. The type and orientation of reinforcement had some effect on the yield and tensile strengths of the composites, but only for those in which the whiskers were more highly oriented. The effect was not general. This suggests that, with the current state of the art in materials and fabrication development, particulate and nodule reinforcements are as effective as whisker reinforcement. Higher failure strains were observed in composites tested in this study than in most previous studies. This increase in ductility was attributed to purer, more uniform starting materials and to more mechanical working during fabrication. Comparing mechanical properties with those of other aluminum alloys showed that these low-cost, lightweight composites demonstrate very good potential for application to aerospace structures.

17. Key Words (Suggested by Author(s))	18. Distribution Statement
Composite material; Metal matrix composite; Silicon carbide; Whisker; Nodule; Particulate; Aluminum; Stress-strain behavior	Unclassified - unlimited STAR Category 23

19. Security Classif. (of this report)	20. Security Classif. (of this page)	21. No. of pages	22. Price*
Unclassified	Unclassified	31	A03

*For sale by the National Technical Information Service, Springfield, Virginia 22161

NASA-Langley, 1984

National Aeronautics and
Space Administration

Washington, D.C.
20546

Official Business
Penalty for Private Use, $300

THIRD-CLASS BULK RATE

Postage and Fees Paid
Nati
Spa
NAS

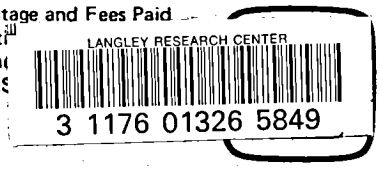

NASA

POSTMASTER: If Undeliverable (Section 158 Postal Manual) Do Not Return